Excretion through digestive tissues predates the evolution of excretory organs

Carmen Andrikou[1], Daniel Thiel[1], Juan A. Ruiz-Santiesteban[1], Andreas Hejnol[1*]

[1]Sars International Centre for Marine Molecular Biology, University of Bergen, Thormøhlensgate 55, 5006 Bergen, Norway

Corresponding author: andreas.hejnol@uib.no

Excretory organs such as nephridia and kidneys are seen as a nephrozoan novelty since they are neither present in Xenacoelomorpha (*Xenoturbella* + Acoelomorpha) nor outside Bilateria. However, the evolutionary origin of excretory organs and the ancient mode of excretion before their existence remain unclear. In this study we investigated the excretion in an acoel and a nemertodermatid, both members of the Xenacoelomorpha, the sister group to all remaining Bilateria (fish, frogs, humans). We examined the expression of excretion-related genes associated with the different compartments of nephridia (ultrafiltration-affiliated genes, rootletin, solute carrier transporters, aquaporins) and genes involved in ammonia excretion (Rhesus, Na^+/K^+ ATPase, v-ATPase and Carbonic Anhydrase). We show that in acoelomorphs the ultrafiltration-affiliated genes have a broad expression while most of the other excretion-related genes are expressed in defined domains neighboring the reproductive and digestive systems. These domains are spatially unrelated to nephridial compartments of other Bilateria. Our experimental approach indicates that Na^+/K^+ ATPase, v-ATPase and Rhesus proteins are involved in the active ammonia excretion mechanism in acoels, contrary to the previously hypothesized excretion by passive diffusion. To test if we find similar mechanisms outside Bilateria, we extended our study to the cnidarian *Nematostella vectensis* and show that also in this group the ammonia excretion-related genes are expressed in gastrodermal domains. Together, our results suggest that in acoelomorphs and cnidarians excretion takes place through digestive-tissues and that this mode of excretion might have been the major excretory mechanism present before the specialized excretory organs of animals evolved.

Introduction

Excretory organs are specialized organs that remove the metabolic waste products and control the water and ion balance in the organism (1). They generally function using the principles of ultrafiltration, absorption and secretion. Ultrafiltration is based on a concentration-driven separation of

molecules and requires a filter-like membranous structure and hydrostatic or osmotic pressure. Absorption and secretion occur via passive and active transport mechanisms, which involve passive diffusion and trans-membranous transporters (2). Depending on the principles they use, excretory organs can be categorized in nephridia, which combine all these basic principles, and other taxon-specific excretory organs, which perform either ultrafiltration (such as the nephrocytes of insects (3) and the rhogocytes of gastropods (4)), or absorption and secretion via transporters such as the malpighian tubules of tardigrades, arachnids and insects (5-11) and the Crusalis organs of copepods (12). However, most main bilaterian lineages possess nephridia (1). Based on morphological correspondences they can be grouped in two major architectural units: the protonephridia, only found in Protostomia, and the metanephridia, present in both Deuterostomia and Protostomia (which together form the Nephrozoa (13)) (Fig. 1A). Both types of organs are organized into functionally similar compartments: The terminal cells of protonephridia and the podocytes of metanephridia conduct ultrafiltration and the tubule and duct cells perform a series of selective reabsorption and secretion of the filtrate, followed by the elimination of the final excrete through the nephropore to the exterior of the animal. The main difference between protonephridia and metanephridia is whether their proximal end is blind-ended or not, respectively (14, 15).

The origin and the homology of excretory organs are unsolved (1, 14, 16-20). Interestingly, recent molecular studies have shown that a number of orthologous developmental (e.g. *hunchback, sall, osr, pou2.3, six1/2, eya etc*) and structural genes (*nephrocyctins, rootletin*) as well as a group of ion transporters (solute carrier transporters (SLCs)) are spatially expressed in a corresponding manner in the tubule and the duct cells of protonephridia of planarians and the metanephridia of vertebrates (21-23) (Fig. 1B). Also, ammonia-secretion related genes encoding the Rhesus and Na^+/K^+ ATPase transporters, the vacuolar H^+-ATPase proton pump (a and b subunits) and the Carbonic Anhydrase A (2 and 4 members) are expressed in excretion sites of several nephrozoans, regardless whether they possess specialized excretory organs (24-35) or not (36, 37) (Fig. 1C). Moreover, a suite of orthologous structural membrane-associated genes (*nephrin/kirre, cd2ap, zo1, stomatin/podocin*) is expressed at the ultrafiltration site of the slit diaphragm of the rodent podocytes (38) and the *Drosophila* nephrocytes (39). *Nephrin/kirre* is also expressed at the ultrafiltration site of the planarian terminal cells (23), as well as the gastropod rhogocytes (4) (Fig. 1B).

Since there is only little information about the excretory modes outside Nephrozoa, it is not known whether the spatial assembly of these genes in defined excretory sites occurred before the emergence of specialized excretory organs. Most of the nephridia-associated solute carrier transporters (slc4, slc9, slc12, slc13 and slc26) as well as the water/glycerol/ammonia channels (aquaporins) (40, 41) are also present in plants (42), where they control osmoregulation and metabolism. All four ammonia

excretion-related components (rhesus/amt, Na^+/K^+ ATPase transporters, vacuolar H^+-ATPases and carbonic anhydrases) also have an ancient origin, as they are found in Eubacteria (43-46), where they have roles in osmoregulation, proton pumping and CO_2 fixation, respectively. Finally, the integral membrane protein stomatin is widely distributed on the phylogenetic tree including Archaea (47), and the membrane associated guanylate kinase (MAGUK) protein zo1 roots back to the protist *Capsaspora owczarzaki* (48). To better understand the excretory mechanisms outside Nephrozoa and their relevance for the evolution of excretory organs, an investigation of the aforementioned genes in a non-nephrozoan group with an informative phylogenetic position is necessary.

Xenacoelomorpha (*Xenoturbella* + (Nemertodermatida + Acoela)) are bilaterally symmetric, small acoelomate aquatic worms that have been shown to be the sister group of Nephrozoans (13, 49-52). They are hermaphroditic and have paired, non-epithelial gonads consisting of ventral ovaries and dorsolateral testes. They live in benthic or interstitial microhabitats and their gut has a single opening, the mouth, which is located ventrally (summarized in (53, 54)). Most Acoela possess a syncytial, lumen-less gut, into which they ingest by phagocytosis whereas *Xenoturbella*, Nemertodermatida and the acoel *Paratomella* have epithelia-lined, cellular guts (55, 56); thus, the syncytial condition of the acoel gut does not represent an ancestral character of Xenacoelomorpha (57). Unlike in other small, meiofaunal animals, neither excretory organs nor defined excretory structures have been described for xenacoelomorphs, with the only exception of unique specialized cells with a possible excretory function (dermonephridia) in the acoel group *Paratomella* (58). Also, nothing is known about the excretion mechanism of xenacoelomorphs. Since Xenacoelomorpha is the sister group to Nephrozoa, excretory organs likely appeared after the split of bilaterians into xenacoelomorphs and nephrozoans. Therefore, their key phylogenetic position makes them an informative group for reconstructing the ancestral bilaterian excretory mechanisms and for better understanding the evolutionary origin of specialized excretory organs.

Here, we followed a candidate gene approach and we revealed the expression of excretion-related genes in two representatives of xenacoelomorphs, the acoel *Isodiametra pulchra* (Fig. 1D), that has a syncytial, lumen-less gut and the nemertodermatid *Meara stichopi* (Fig. 1E) with an epithelia-lined gut. We then refined our findings with functional analysis experiments in *I. pulchra* by applying pharmaceutical inhibitors against molecules involved in ammonia transport. Finally, to test whether our observations extend outside Bilateria, we expanded our study to another non-nephrozoan group and sister group to bilaterians, the cnidarians. Our results show that the putative excretory domains in the two acoelomorphs and the cnidarian *Nematostella vectensis* are in close proximity to the reproductive and digestive systems and therefore suggest that in these taxa, excretion likely occurs

through the gastric cavity. This mode of excretion might have been commonly used in animals before the emergence of specialized excretory organs in Nephrozoa.

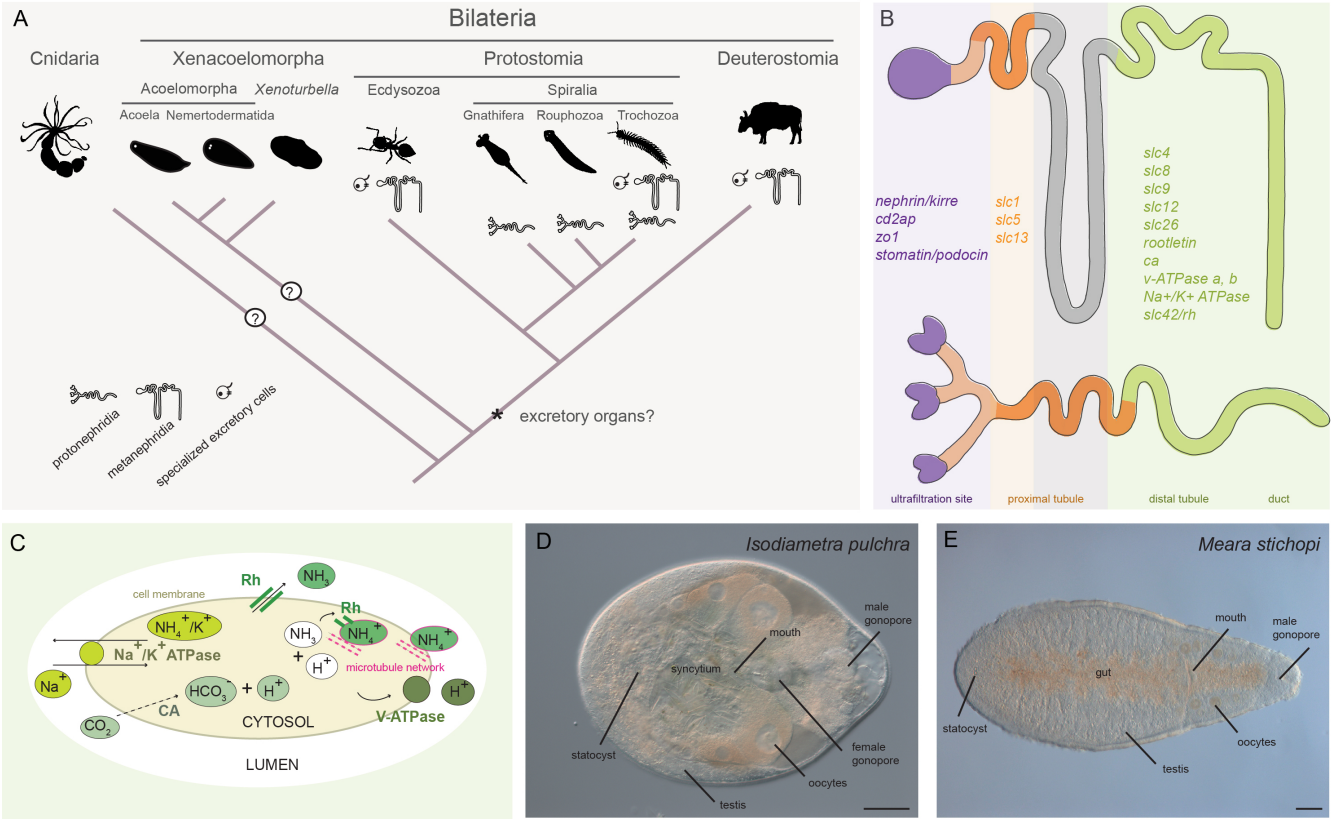

Figure 1. Phylogenetic distribution of excretory organs, structural and functional correspondence of protonephridial and metanephridial domains and ammonia excretion mechanism. (A) Illustrated phylogenetic relationship between Nephrozoa, Xenacoelomorpha and Cnidaria. Excretory organs or specialized excretory cells/tissues are so far only reported in the group of Nephrozoa. Animal illustrations are taken from phylopic.org (B) Cartoon depiction of the structural components of metanephridia in comparison to protonephridia and summary of the expression domains of orthologous selected genes in relation to their components. (C) Ammonia cellular transport. Ammonia (NH_3) is secreted into the lumen fluid via parallel H^+ and ammonia transport. This involves direct transport through the Rhesus glycoproteins (Rh), the active Na^+/K^+ ATPase as well as the generation of H^+ gradient by a v-ATPase and the carbonic anhydrase (CA), which transforms CO_2 into H^+ and HCO_3^-. Vesicular ammonia-trapping mechanism is also illustrated. Pictures of the acoelomorph representatives (D) *Isodiametra pulchra* (scale bar = 50 µm) and E) *Meara stichopi* (scale bar = 100 µm).

Materials and Methods

Gene cloning and orthology assignment

Putative orthologous sequences of genes of interest were identified by tBLASTx search against the transcriptome (SRR2681926) of *Isodiametra pulchra*, the transcriptome (SRR2681155) and draft genome of *Meara stichopi* and the genome of *Nematostella vectensis* (http://genome.jgi.doe.gov). Additional transcriptomes of Xenacoelomorpha species investigated were: *Childia submaculatum* (Acoela) (SRX1534054), *Convolutriloba macropyga* (Acoela) (SRX1343815), *Diopisthoporus*

gymnopharyngeus (Acoela) (SRX1534055), *Diopisthoporus longitubus* (Acoela) (SRX1534056), *Eumecynostomum macrobursalium* (Acoela) (SRX1534057), *Hofstenia miamia* (Acoela) (PRJNA241459), *Ascoparia* sp. (Nemertodermatida) (SRX1343822), *Nemertoderma westbladi* (Nemertodermatida) (SRX1343819), *Sterreria* sp. (Nemertodermatida) (SRX1343821), *Xenoturbella bocki* (Xenoturbella) (SRX1343818) and *Xenoturbella profunda* (Xenoturbella) (SRP064117). Gene orthology of the retrieved sequences was tested by reciprocal BLAST against NCBI Genbank followed by phylogenetic analyses. Amino acid alignments were made with MUSCLE (NEXUS files are available upon request). RAxML (version 8.2.9) was used to conduct a Bayesian phylogenetic analysis. Fragments of the genes of interest were amplified from cDNA of *I. pulchra*, *M. stichopi* and *N. vectensis* by PCR using gene specific primers. PCR products were purified and cloned into a pGEM-T Easy vector (Promega, USA) according to the manufacturer' s instruction and the identity of inserts confirmed by sequencing. Primer sequences are available on request. Gene accession numbers are listed in the Supplementary Table 2.

Animal husbandry

Adult specimens of *Isodiametra pulchra* (Smith & Bush, 1991) (59) were kept as previously described (60). *Meara stichopi,* Westblad, 1949 (61) adults were collected and handled as previously described (62). *Nematostella vectensis,* Stephenson, 1935 (63) were kept and handled as previously described (64).

Whole Mount In Situ Hybridization

Animals were manually collected, fixed and processed for in situ hybridization as described by (65). Labeled antisense RNA probes were transcribed from linearized DNA using digoxigenin-11-UTP (Roche, USA), or labeled with DNP (Mirus, USA) according to the manufacturer's instructions. For *I. pulchra* and *M. stichopi*, colorimetric Whole Mount In Situ Hybridization (WMISH) was performed according to the protocol outlined in (65). For *N. vectensis*, we followed the protocol described by (66). Double Fluorescent In Situ Hybridization (FISH) was performed as the colorimetric WMISH with the following modifications: After the post-hybridization steps, animals were incubated overnight with peroxidase-conjugated antibodies at 4°C (anti-DIG-POD, Roche 1:500 dilution and anti-DNP, Perkin Elmer, 1:200 dilution) followed by the amplification of the signal with fluorophore-conjugated tyramides (1:100 TSA reagent diluents, Perkin Elmer TSA Plus Cy3 or Cy5 Kit). Residual enzyme activity was inhibited via 45-minute incubation in 0.1% hydrogen peroxide in PTW followed by four PTW washes prior to addition and development of the second peroxidase-conjugated antibody (67).

Whole Mount Immunohistochemistry

Animals were collected manually, fixed in 4% paraformaldehyde in SW for 1 hour, washed 3 times in PBT and incubated in 4% sheep serum in PBT for 30 min. The animals were then incubated with commercially available primary antibodies (anti-RhAG (ab55911) rabbit polyclonal antibody, diluted 1:50 (Abcam, USA), anti-Na/K ATPase (a1 subunit) rat monoclonal antibody, dilution 1:100 (Sigma-Aldrich, USA) and anti-v-ATPase B1/2 (L-20) goat polyclonal antibody, dilution 1:50 (Biotechnology, Santa Cruz, USA) overnight at 4°C, washed 10 times in PBT, and followed by incubation in 4% sheep serum in PBT for 30 min. Specimens were then incubated with a secondary antibody (anti rabbit-AlexaFluor 555, Invitrogen or anti rat-AlexaFluor555 and anti goat-AlexaFluor555) diluted 1:1000 overnight at 4°C followed by 10 washes in PBT. Nuclei were stained by incubation of animals in DAPI 1:1000 and f-actin was stained by incubation in BODIPY labeled phallacidin 5 U/ml overnight.

Inhibitor experiments

For excretion experiments approximately 250 fed animals were placed into glass vials with 2 ml UV sterilized natural seawater, containing the appropriate inhibitor or ammonia concentration. Animals were given 10 minutes to adjust to the medium before the solution was exchanged with 2 ml of fresh medium with the same appropriate condition. After 2 hours of incubation the medium was removed and stored at -80°C for later measurements. Animals from the high environmental ammonia (HEA) experiments were then rinsed 5 times and incubated for another 2 hours in fresh seawater without additional ammonia.

We tested different inhibitor concentrations that were used in previous studies in other invertebrates (25, 29, 30, 36, 68). The concentrations of 5 µM Concanamycin C for inhibiting v-ATPase a/b, 1 mM Azetazolamide as an inhibitor of the carbonic anhydrase A 2, 1 mM Quabain to inhibit the Na^+/K^+ ATPase and 2mM Colchicine for inhibiting the microtubule network were selected as the lowest that enabled the observation of a phenotype. Quabain was diluted in DMSO with a final concentration of 0.5% DMSO per sample for which we used an appropriate seawater control with 0.5% DMSO. For the HEA experiments we enriched seawater with NH_4Cl to the final ammonia concentrations of 50 µM, 100 µM, 200 µM and 500 µM. All experiments were performed twice with different animals and the change in excretion rate was tested for significance with an unpaired t-test.

Determination of ammonia excretion

Ammonia concentrations were measured with an ammonia sensitive electrode (Orion, Thermo Scientific) according to (69). Total ammonia was transformed into gaseous NH_3 by adding 54 µl ionic

strength adjusting solution (1.36 ml/l trisodiumcitrate dihydrate, 1 M NaOH) to 3.6 ml of sample. Samples were diluted 1:4 with distilled water to prevent salt precipitation. Due to the small ammonia concentrations the electrode-filling solution was diluted to 10% with distilled water, as suggested in the electrode manual. Solutions with defined ammonia concentrations for the standard curves were made together with the solutions used in the experiments and stored in a similar way at -80°C. For the standard curve we used the following concentrations: 1 µM, 2.5 µM, 5 µM, 10 µM, 17.5 µM, 25 µM, 37.5 µM, 50 µM, 75 µM, 100 µM.

Documentation

Colorimetric WMISH specimens were imaged with a Zeiss AxioCam HRc mounted on a Zeiss Axioscope A1 equipped with Nomarski optics and processed through Photoshop CS6 (Adobe). Fluorescent-labeled specimens were analyzed with a SP5 confocal laser microscope (Leica, Germany) and processed by the ImageJ software version 2.0.0-rc-42/1.50d (Wayne Rasband, NIH). Figure plates were arranged with Illustrator CS6 (Adobe).

Results

Excretion-related gene complement

We focused on three different groups of genes, which are reported to be involved in excretion:

1.) genes encoding proteins that form the ultrafiltration sites of the vertebrate terminal cells, planarian podocytes, insect nephrocytes and gastropod rhogocytes (*nephrin/kirre, cd2ap, zo1* and *stomatin/podocin*) (4, 23, 39);

2.) genes expressed in the nephridia tubule and duct-associated cells composed of **a**) structural genes (*rootletin*) and **b**) solute carrier transporters (*slc1* (glutamate/neutral amino acid transporters), *slc4* ($HCO3^-$ transporters), *slc5* (Na^+/Glucose transporters), *slc8* ($Na^+/Ca2^+$ exchangers), *slc9* (Na^+/H^+ exchangers), *slc12* ($Na^+/K^+/2Cl^-$ cotransporters), *slc13* (Na^+-sulfate(NaS)/carboxylate(NaC) cotransporters), *slc26* (multifunctional anion transporters)) in vertebrates and planarians (21-23) as well as *aquaporins* (water/glycerol/ammonia transporters widely distributed on the phylogenetic tree with an osmoregulatory function (41));

3.) genes involved in ammonia excretion in several nephrozoans (*slc42/rhesus* (ammonia transporters), *Na^+/K^+ ATPase, v-ATPase a, b* and *carbonic anhydrase A 2, 4*) and expressed both in tubule and duct-associated cells of nephridia and in taxon-specific excretory organs or excretory structures (24-36).

We searched for orthologous sequences of these genes in available transcriptomes of 13

xenacoelomorph species (*Isodiametra pulchra, Hofstenia miamia, Convolutriloba macropyga, Diopisthoporus longitubus, Diopisthoporus gymnopharyngeus, Eymecynostomum macrobursalium, Childia submaculatum, Meara stichopi, Nemertoderma westbladi, Sterreria* sp., *Ascoparia* sp., *Xenoturbella bocki* and *Xenoturbella profunda*), the cnidarian *Nematostella vectensis*, the placozoan *Trichoplax adhaerens,* the sponge *Amphimedon queenslandica,* the ctenophore *Mnemiopsis leidy,* the protist *Capsaspora owczarzaki,* the amoeba *Dictyostelium discoideum* and the nephrozoans *Homo sapiens, Saccoglossus kowalevskii, Strongylocentrotus purpuratus, Xenopus laevis, Branchiostoma lanceolatum*, *Capitella teleta, Crassostrea gigas, Lottia gigantea, Schmidtea mediterranea, Tribolium castaneum, Caenorhabditis elegans* and *Drosophila melanogaster*. We found that representatives from *cd2ap, stomatin/podocin, slc4, slc9, slc12, slc13, slc26, aquaporin, carbonic anhydrase A, v-ATPase, rh, amt* and Na^{+}/K^{+} *ATPase* were present in almost all groups. *Slc1* was only found in metazoans (with the exception of *Mnemiopsis leidy),* however (70) reported its presence in the archaean *Pyrococcus horikoshi,* Sequences for *nephrin/kirre* were only present in Xenacoelomorphs and Nephrozoa, indicating that they originated within the Bilateria. *Zo1* was only present in *Capsaspora owczarzaki* and most metazoans, suggesting that it originated within the Holozoa, as proposed already by (48). *Rootletin* and *slc5* were only found in Planulozoa. *Slc8* was only present in *Capsaspora owczarzaki, Trichoplax adhaerens* and Planulozoa, but (71) reported its presence in the archaean *Methanococcus jannaschii* (Fig. 2). The orthology of the retrieved sequences was assessed with phylogenetic analyses (Supplementary Fig. S1). The expression/role of the excretion-related genes in metazoan and non-metazoan taxa is summarized in Supplementary Table 1.

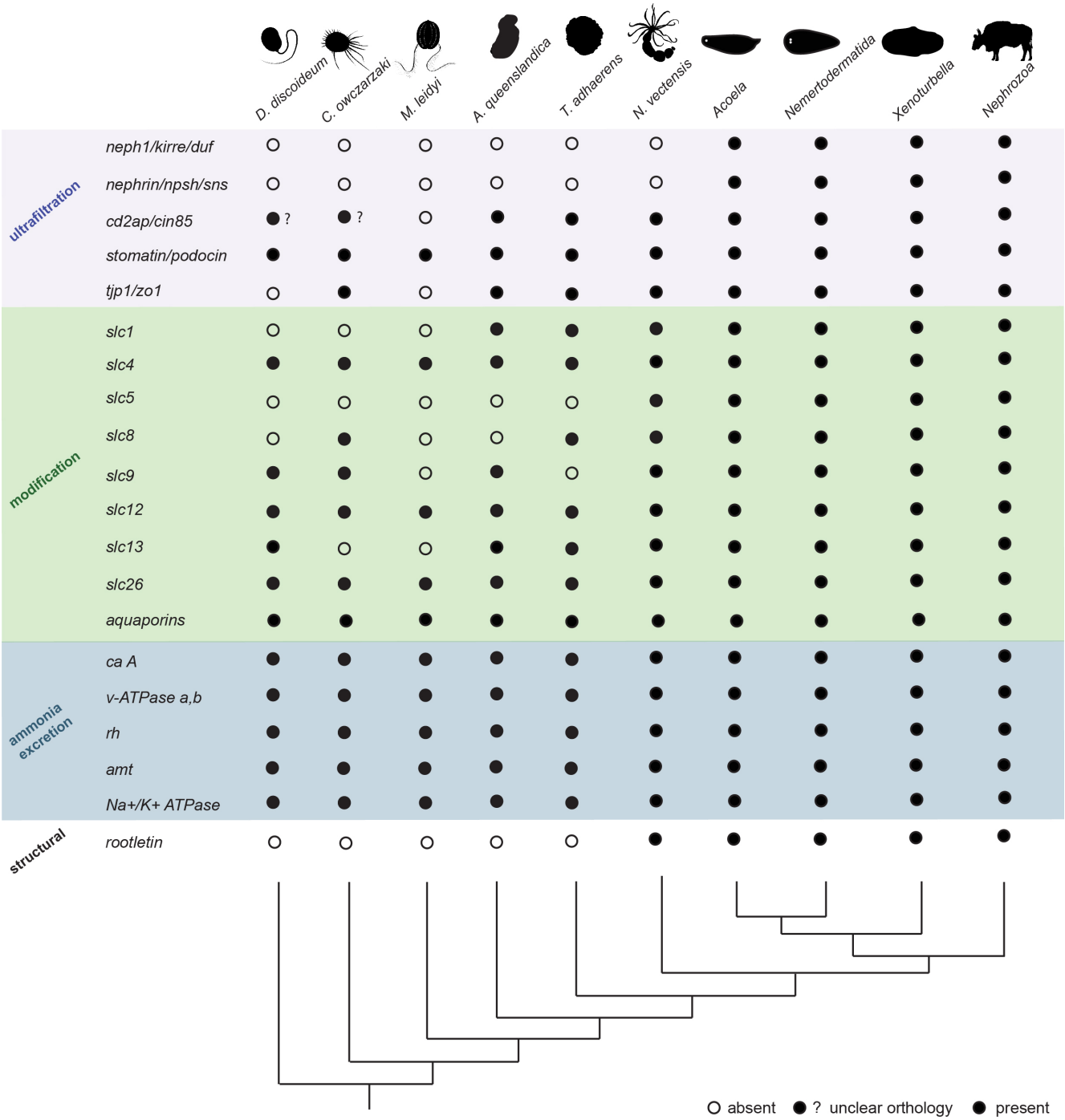

Figure 2. Excretion-related gene complement in *Dictyostelium discoideum, Capsaspora owczarzaki, Trichoplax adhaerens, Mnemiopsis leidyi, Amphimedon queenslandica, Nematostella vectensis* as well as in members of Acoela, Nemertodermatida, Xenoturbella and Nephrozoa.

Transriptome and genome mining of excretion-related gene repertoire in *Dictyostelium discoideum,* as a representative of Amoebozoa, *Capsaspora owczarzaki,* as a representative of Filasterea, *Trichoplax adhaerens,* as a representative of Placozoa, *Mnemiopsis leidyi,* as a representative of Ctenophora, *Amphimedon queenslandica,* as a representative of Porifera, *Nematostella vectensis,* as a representative of Cnidaria, *Isodiametra pulchra, Hofstenia miamia, Convolutriloba macropyga, Diopisthoporus longitubus, Diopisthoporus gymnopharyngeus, Eymecynostomum macrobursalium* and *Childia submaculatum,* as representatives of Acoela, *Sterreria* sp., *Ascoparia* sp., *Meara stichopi* and *Nemertoderma westbladi,* as representatives of Nemertodermatida, *Xenoturbella bocki* and *Xenoturbella profunda,* as representatives of Xenoturbella and the deuterostomes *Homo sapiens, Saccoglossus kowalevskii, Strongylocentrotus purpuratus, Xenopus laevis, Branchiostoma lanceolatum* and protostomes *Capitella teleta, Crassostrea gigas, Lottia gigantea, Schmidtea mediterranea, Tribolium castaneum, Caenorhabditis elegans* and *Drosophila melanogaster,* as representatives

of Nephrozoa. Data are based on this study unless stated otherwise.

Identification and characterization of excretion-related genes in *I. pulchra* and *M. stichopi*

Sequences for all genes were detected in the transcriptomes of the acoel *I. pulchra* and the nemertodermatid *M. stichopi* and in most cases more than one gene copy was revealed. Their spatial expression was further analyzed by WMISH.

Nephrin/kirre, cd2ap, zo1 and stomatin/podocin are broadly expressed in acoelomorphs

In the *I. pulchra* transcriptome, three *nephrin/kirre*, one *cd2ap*, one *zo1* and three *stomatin/podocin* genes, orthologous to *H. sapiens stomatin3/podocin* group, (Supplementary Fig. S1) were found. *Nephrin/kirre* genes showed diverse expression patterns; *nephrin/kirre a* was expressed in the female gonadal region and in two lateral rows of cells at the posterior end (Fig. 3A), *nephrin/kirre b* was restricted in lateral parenchymal cells that resembled neurons (Fig. 3B) and *nephrin/kirre c* was localized in the oocytes and in cells at the anterior end (Fig. 3C). Both *cd2ap* and *zo1* were detected in the female gonadal region and in lateral parenchymal cells (Fig. 3D-E). *Zo1* was further expressed in cells at the anterior and posterior end (Fig. 3E). *Stomatin/podocin* genes exhibited diverse expression patterns; *stomatin/podocin a* was localized around the digestive syncytium and strongly in two flame-like cells laterally adjacent to the anterior part of the syncytium (Fig. 3F), *stomatin/podocin b* was expressed in the female gonadal region and around the digestive syncytium with expression more prominent at the anterior part (Fig. 3G) and *stomatin/podocin c* was broadly detected in the parenchyma, around the digestive syncytium, the female gonadal region, and cells at the anterior and posterior end (Fig. 3H). Together, these data show that the ultrafiltration-related genes are expressed in several domains in *I. pulchra* including anterior, posterior, possible neuronal, gonadal, parenchymal and syncytium-associated domains.

In the *M. stichopi* transcriptome, three *nephrin*/*kirre*, one *cd2ap*, one *zo1* and five *stomatin/podocin* genes, orthologous to *H. sapiens stomatin3/podocin* group, (Supplementary Fig. S1) were identified. All three *nephrin*/*kirre* genes were localized in different types of subepidermal cells (Fig. 3A'-C') whilst *nephrin*/*kirre a* and *b* were further expressed in gut lining cells (Fig. 3A'-B'). *Nephrin*/*kirre a* exhibited an additional expression domain in the region of female gonads (Fig. 3A'). *Cd2ap* exhibited a broad expression, including scattered cells of the subepidermis, cells at the anterior end, female gonadal region and the mouth region (Fig. 3D') and *zo1* was expressed in the gut epithelum, cells at the anterior end, the mouth, the female gonadal region and two proximal lateral rows of cells neighboring the gut (Fig. 3E'). *Stomatin/podocin genes* showed diverse expression patterns; *stomatin/podocin a* was localized in distal lateral rows of subepidermal cells and testis (Fig. 3F'),

stomatin/podocin b was ubiquitously expressed including two distal lateral rows of subepidermal cells, the mouth and cells at the anterior end (Fig. 3G'), *stomatin/podocin c* was expressed in scattered subepidermal cells and individual cells near the gut (Fig. 3H'), *stomatin/podocin d* was broadly expressed in the epidermis (Supplementary Fig. S3a) and *stomatin/podocin e* in subepidermal cells (Supplementary Fig. S3b). These findings show that the ultrafiltration-related genes are also demarcating various domains in *M. stichopi* including anterior, posterior, subepidermal, gonadal, distal lateral subepidermal and gut-associated regions.

Slc transporters, aquaporins and rootletin are mainly expressed in neuronal, gonadal, gut-associated and parenchymal domains in acoelomorphs

Transporters expressed in the proximal tubule cells of nephridia (*slc1, slc5* and *slc13*) were expressed in several domains in *I. pulchra*. Three *slc1* paralogs, two *slc5* and one *slc13* were found in *I. pulchra* transcriptome. *Slc1 a*, *b* and *slc5* were mainly expressed in the lateral parenchyme and the female gonadal region (Fig. 3I-J). *Slc1 a* and *b* were additionally expressed in cells around the statocyst (*slc1 a* shown, Fig. 3I). *Slc13* was detected in the lateral parenchyme and in cells around the statocyst (Fig. 3K). These results show that the proximal tubule-related genes are localized in anterior, gonadal and parenchymal domains in *I. pulchra.*

In *M. stichopi* transcriptome one *slc1*, two *slc5* and four *slc13* were detected. Both *slc5* paralogs were expressed in individual scattered cells near the gut, in the region of female gonads and in two distal lateral rows of subepidermal cells in *M. stichopi* (Fig. 3J'). *Slc13 a, b, c* and *d* were all labeling individual subepidermal cells, possibly neurons (*slc13 a* shown, Fig. 3K'). These data show that the proximal tubule-related genes are expressed in possibly neuronal, gonadal, gut lining as well as distal lateral subepidermal domains in *M. stichopi.*

The genes localized in the nephridial distal tubule and duct (*slc4, slc9, slc12, slc26, slc8, aquaporins and rootletin*) were expressed in various domains in *I. pulchra*. Three *slc4* paralogs were found in the transcriptome of *I. pulchra*. *Slc4 a* was expressed in cells at the anterior end, the female gonadal region and in lateral parenchymal cells (Fig. 3L), *slc4 b* was expressed ubiquitously (Supplementary Fig. S2a) and *slc4 c* was confined in the oocytes (Supplementary Fig. S2b). *Slc9* transcripts were localized in parenchymal cells surrounding the mouth and in two lateral domains posterior of the mouth (Fig. 3M). Two copies of *slc12* were detected: *slc12 a* was expressed broadly including the female gonadal region, the lateral parenchyme and the anterior end (Fig. 3N) whilst *slc12 b* expression was only seen in the oocytes (see Supplementary Fig. S2c). No expression of *slc26 a* was detected (Fig. 3O). *Slc8* was localized in the female genital opening, in cells at the anterior end and faintly in the female gonadal region (Fig. 3P). Seven aquaporin genes were found and the expression patterns of

aquaporin a (I. pulchra specific aquaporin), *aquaporin b* (orthologous of *H. sapiens aq 8*), *aquaporin c* and *aquaporin d* (orthologous of *H. sapiens aq 3,7,9,10,11,12*) (Supplementary Fig. S1) were revealed. *Aquaporin a* was expressed around the digestive syncytium and its expression domain was more prominent at the anterior part (Supplementary Fig. S2d), *aquaporin b* was localized in parenchymal cells bordering the testis and the region of female gonads (Supplementary Fig. S2e). *Aquaporin c* and *d* were both localized in the testis (Supplementary Fig. S2f-g). *Rootletin a* was exclusively expressed in the female gonadal region and the oocytes (Supplementary Fig. S2h). All together, these results show that the tubule and duct-related genes are expressed in anterior, gonadal, parenchymal and syncytial-associated domains in *I. pulchra*.

Similarly, the orthologous genes localized in the nephridial distal tubule and duct showed a broad expression in *M. stichopi.* From the three *slc4* paralogs, *slc4a* was localized in scattered subepidermal cells, in two posterior distal lateral rows of subepidermal cells and in cells at the anterior end (Fig. 3L'); *slc4 b* was expressed in distinct scattered cells near the gut and around the mouth (Supplementary Fig. S3c) and *slc4 c* was confined in two proximal lateral rows of cells (Supplementary Fig. S3d). *Slc9* was localized in the gut epithelium and in two posterior proximal lateral rows of cells neighboring the gut (Fig. 3M'). Three *slc12* genes were identified in *M. stichopi* transcriptome and the expression of *slc12 a* and *b* were revealed. Both genes showed a similar expression in distinct cells of the gonadal region and in the cells surrounding the gut lumen (Fig. 3N'). Two *slc26* genes were revealed: *slc26 a* expression was restricted in the region of female gonads (Fig. 3O') whilst *slc26 b* was localized both in male and female gonadal region (Supplementary Fig. S3e). *Slc8* was exclusively expressed in two proximal posterior lateral rows neighboring the gut (Fig. 3P'). Six aquaporin genes were found in *M. stichopi* transcriptome; *aquaporins a, d, f,* (orthologous of *H. sapiens aq 2,4,5,6*), *b, e* (orthologous of *H. sapiens aq 8*) and *c* (orthologous of *H. sapiens aq 3,7,9,10*) (Supplementary Fig. S1). Both *aquaporins a* and *b* were expressed in individual scattered cells near the gut and in the region of female gonads, however the expression of *aquaporin a* extended more anteriorly compared to *aquaporin c* (Supplementary Fig. S3f-g). *Aquaporin c* and *aquaporin d* were also detected in gut-lining cells but the two domains were different: *aquaporin c* was expressed in gut-lining cells towards the midline of the gut whilst *aquaporin d* was localized in distal gut-lining cells (Supplementary Fig. S3h-i). *Aquaporin c* was additionally expressed in two proximal lateral rows lining the gut (Supplementary Fig. S3h). *Aquaporin e* was localized in the ventral epidermis (Supplementary Fig. S3j) whilst *aquaporin f* had a faint ubiquitous expression with a stronger domain of expression in two distal lateral rows of subepidermal cells (Supplementary Fig. S3k). *Rootletin* was localized in individual scattered cells near the gut, with a tubular structure, and the male gonopore (Supplementary Fig. S3l). These findings show that in *M. stichopi* the tubule and duct-related genes

are demarcating epidermal, subepidermal, possibly neuronal, gonadal, distal lateral subepidermal, gut-lining as well as proximal lateral gut-neighboring domains.

Rhesus, carbonic anhydrase A, Na^+/K^+ ATPase and v-ATPase a, b are mainly expressed in gut and gonad associated domains in acoelomorphs

In *I. pulchra,* the analyzed orthologs of genes with a conserved role in ammonia transport mechanism (*Rhesus* and *v-ATPase a, b*) were mainly expressed in domains in proximity to the digestive system and gonads. *Rh* was exclusively expressed in parenchymal cells bordering the digestive syncytium (Fig. 3Q). We studied also the expression of amts (ammonia transporters) since they are homologs of Rh proteins (72, 73). Six amts were found in the *I. pulchra* transcriptome*; amt 1* and *amt 3* (orthologs of *C. elegans amt 1/4*) and *amt4*, *amt 5* and *amt6* (orthologs of *C. elegans amt 2/3*) (Supplementary Fig. S1). *Amt1* exhibited a broad pattern of expression including the female gonadal region and in lateral parenchymal cells, *amt 2* was localized in the female gonadal region and *amt 3* and *4* were confined in the oocytes, *amt 5* expression was limited in the testis and *amt 6* was broadly detected in the parenchyma and in posteriorly placed cells around the male gonopore (Supplementary Fig. S2i-n). *V-ATPase a* and *v-ATPase b* were both strongly expressed in the digestive syncytium (Fig. 3R-S). *V-ATPase b* was further expressed and in few cells at the posterior tip (Fig. 3S). Both *Na^+/K^+ ATPase* paralogs found in *I. pulchra* transcriptome were exclusively expressed in the testis (Fig. 3T). Nine copies of *ca a* were found in *I. pulchra* transcriptome and the expression patterns of *ca a1, ca a2, ca a3* and *ca a4* (orthologous to *H. sapiens ca a* 4,6,9,12,14) and *ca a5* (orthologous to *H. sapiens ca a* 1,2,3,5,7,8,13) (Supplementary Fig. S1) were revealed. *Ca a1* was expressed in few distal cells at the anterior end, cells at the posterior tip around the male gonopore, gonads and ventral parenchymal cells neighboring the digestive syncytium (Fig. 3U), *ca a2* was localized in cells at the anterior end, the female gonadal region and lateral parenchymal cells (Fig. 3V) whilst the expression of *ca a3* and *ca a4* was demarcating cells around the statocyst, female gonadal region and oocytes (Fig. 3W). *Ca a5* was broadly expressed in the parenchyme and more prominently in the region of female gonads (Fig. 3X). Together, these data show in *I. pulchra* the ammonia excretion-related genes are expressed in anterior, posterior, gonadal and syncytium-associated domains.

In *M. stichopi,* the majority of orthologous ammonia excretion–related genes were expressed near the gut. *Rh* was localized broadly, with its expression to be more prominent in scattered subepidermal cells, two posterior distal dorsolateral subepidermal rows of cells and the anterior epidermis (Fig. 3Q'). The single *amt* copy that was detected, orthologous to *C. elegans amt 2/3* (Supplementary Fig. S1), exhibited an expression in epidermal cells (Supplementary Fig. S3m). Both *v-ATPase a* paralogs were localized in the gut epithelium (Fig. 3R' Supplementary Fig. S3n). From the two *v-ATPase b*

genes identified, *v-ATPase b1* was expressed in the gut epithelium in a gradient manner, more prominently at the posterior part, and in two proximal lateral rows of cells lining the gut (Fig. 3S') whilst *v-ATPase b*2 didn't reveal any expression (Supplementary Fig. S3o). Na^+/K^+ *ATPase* was detected in cells adjacent to the gut epithelium with the expression to be more enriched in the posterior part of the gut (Fig. 3T'). Six copies of *ca a* were detected in *M. stichopi* transcriptome and the expression pattern of *ca a1, ca a2* (orthologous to *H. sapiens ca a* 1,2,3,5,7,8,13) and *ca a3, ca a4* (orthologous to *H. sapiens ca a* 4,6,9,12,14) (Supplementary Fig. S1) were revealed. *Ca a1* was localized adjacent to the gut epithelium (Fig. 3U') whilst *ca a2* was expressed in a few scattered gut-lining cells (Fig. 3V'). *Ca a3* was also expressed in the gut epithelium (Fig. 3W') whilst *ca a4* had a broad expression pattern, including gut lining cells, individual lateral cells of the subepidermis, possibly neurons, and the posterior epidermis (Fig. 3X'). These results show that in *M. stichopi* the ammonia excretion-related genes are mainly expressed in gut-associated domains. Other domains revealed were the posterior epidermis, possibly neuronal cells as well as two distal lateral rows of subepidermal cells.

To summarize, the majority of genes analyzed in *I. pulchra* and *M. stichopi* were mainly expressed in gonadal and gut-associated (e.g. mouth, gut-lining cells) or gut-neighboring domains (e.g subepidermal, parenchymal cells, proximal lateral rows of cells). Although the two animals differ significantly in their gut morphology (*I. pulchra* posses a syncytial gut without an epithelium lining whilst *M. stichopi* is characterized by an epithelial branched gut), no major differences were observed regarding the gut-related gene expression apart of the expression of some genes in the gut-epithelium in *M. stichopi* that in *I. pulchra* were either localized in the syncytial cells (e.g *v-ATPase a, b*) or in other regions such as the mouth (e.g. *slc4b* and *slc9*) or the gonads (e.g. *ca a2, a3, a4* and Na^+/K^+ *ATPase*). Additional gene specific domains in *I. pulchra* were scattered cells of the anterior end and laterally placed individual parenchymal cells -likely neurons-, cells in vicinity to the statocyst, the frontal organ, parenchymal cells -likely including muscle cells- as well as cells at the posterior tip often surrounding the male and the female gonopore. In *M. stichopi* additional expression domains revealed were individual cells located at the anterior end, scattered individual subepidermal and distal lateral rows of cells –possibly neurons-, extended subepidermal cells –likely including muscle cells- and cells of the epidermis.

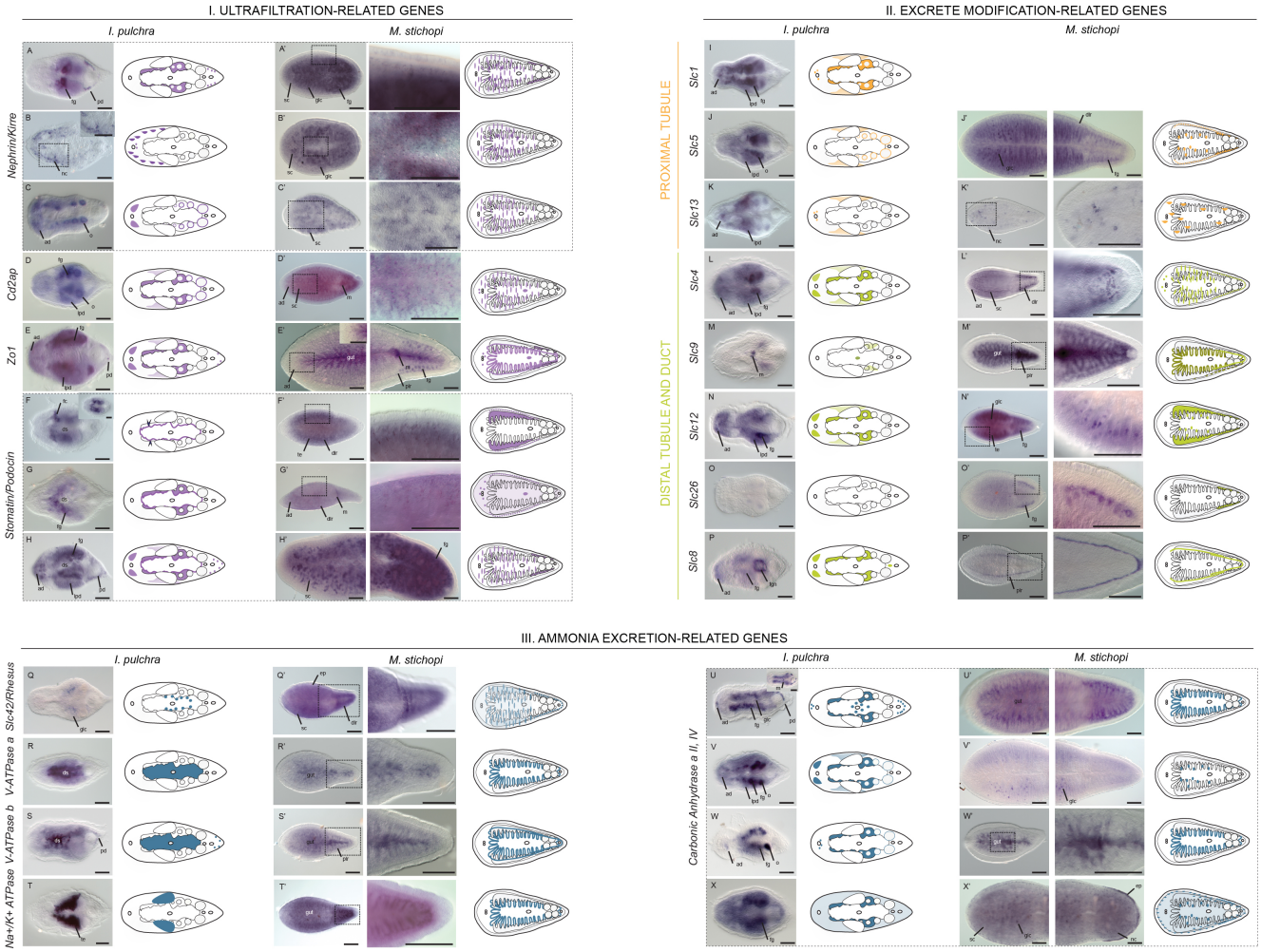

Figure 3. Expression of orthologs of bilaterian excretion-related components in *I. pulchra* and *M. stichopi*. Whole mount in situ hybridization (WMISH) of genes with a known conserved role in excretory organ localization and ammonia excretion. The genes are divided in three groups according to their spatial localization in nephridial compartments. (I) Expression of genes encoding proteins expressed in ultrafiltration sites: *nephrin/kirre, cd2ap, zo1* and *stomatin/podocin*. The inset in panel F shows a different focal plane of the animal, insets in panels B and E' show a higher magnification of the indicated domains and the panels in columns next to A', B', C', D' F' and G' show a higher magnification of the indicated domain in panels A', B', C', D', F' and G', respectively. (II) Expression of genes encoding solute carrier transporters localized both in the tubule and the duct of nephridia: *slc1, slc5* and *slc13* (proximal tubule), *slc4, slc9, slc12, slc26, slc8* (distal tubule and duct). The panels in columns next to K', L', M', N', O' and P' show a higher magnification of the indicated domain in panels K', L', M', N', O' and P', respectively. (III) Expression of genes involved in ammonia excretion in several metazoans: *rh, v-ATPase a* and *v-ATPase b, Na^+/K^+ ATPase* and *carbonic anhydrase A 2, 4*. The inset in panel U shows a different focal plane of the animal, panels in columns next to Q', R', S', T' and W' show a higher magnification of the indicated domain in panels Q', R', S', T' and W', respectively. Illustrations with colored gene expression correspond to the animals shown in the previous column. Anterior is to the left. ad, anterior domain; ds, digestive syncytium; dlr, distal lateral rows; fg, female gonads; fgn, female gonopore; fc, flame-like cells; glc, gut-lining cells; plr, proximal lateral rows; lpd, lateral parenchymal domain; m, mouth; nc, neural cells; o, oocytes; pd, posterior domain; sc, subepidermal cells; te, testis. Scale bars are 50 µm for *I. pulchra* and 100 µm for *M. stichopi*.

Rh protein is present in vesicles localized in the cytoplasm of gut-lining cells in *I. pulchra*

Rh gene expression in *I. pulchra* revealed a group of cells surrounding the gut (Fig. 3Q) but the signal was rather low and the cells did not show any morphological peculiarity by WMISH. In order to obtain a better morphological and spatial resolution of these cells, we revealed the protein localization

of Rh by immunohistochemistry. Rh was exclusively present in individual cells that line the digestive syncytium (Fig. 4A) and have similar characteristics with a specific parenchymal cell type that has previously been characterized as 'gut wrapping-cells' in an Isodiametra species (74). These cells were reported to have a vacuolated cytoplasm, found around the syncytium and sometimes extend processes into it, similar to what was seen in the Rh-expressing cells. Observations with higher magnification showed that Rh transporter was localized in vesicles in the cytoplasm of these cells and not on their surface (Fig. 4A'). These findings show that in *I. pulchra* Rh is not a cellular-membrane transporter but rather a cytoplasmatic-vesicular one thus suggesting that ammonia transport likely occurs through a vesicular-trapping mechanism.

Co-expression of excretion-related genes in *I. pulchra* and *M. stichopi.*

The above spatial analysis revealed explicit expression domains of excretion-related genes in *I. pulchra* and *M. stichopi*, including gonadal, anterior, posterior, subepidermal/parenchymal, gut-associated and gut-neighboring domains. To obtain a better resolution and understanding of the relative topology of these domains, double fluorescent whole mount in situ hybridization (FISH) were conducted for genes encoding proteins generally involved in ammonia excretion (*v-ATPase b, Na^+/K^+ ATPase*, *ca, rh*) and a number of transporters localized in nephridial compartments (24-36) (*slc4, slc9, slc12).* Conserved markers of the germ line and digestive tract were also included in the analysis; *piwi* and *plastin,* respectively (75, 76).

In *I. pulchra, Na^+/K^+ ATPase* and *v-ATPase b* were expressed in a mutually exclusive manner (Fig. 4B). The two domains of expression appeared adjacent to each other; *Na^+/K^+ ATPase* was not expressed in the female gonadal region but exclusively in the testis, as shown by coexpression analysis with *slc4 a* (Fig. 4C), whilst *v-ATPase b* localized all along in the digestive syncytium, as shown by coexpression with *plastin* (Fig. 4D, see also Supplementary Fig. S2o for colorimetric expression of *plastin*). *Slc12 b* was confined in the oocytes whilst *slc4 a* is localized in the region of female gonads around the oocytes (Fig. 4E). *Ca a1* was partly overlapping with *Na^+/K^+ ATPase* but its expression extended more ventrally including the female gonadal region (Fig. 4F). *Ca a1* also labeled cells at the posterior tip and around the male gonopore, cells at the anterior end as well as distinct cells of the ventral surface of the syncytium border and around the mouth (Fig. 4F). These data show a complex arrangement of the expression domains in *I. pulchra,* namely a subdivision of the gut-associated domains in different groups, such as a gut-lining region, a ventral mouth-surrounding region and the digestive syncytium. Similarly, the gonad- associated domains can be subdivided in a testis-restricted region, an oocyte-surrounding region and an oocyte-restricted region.

Similarly, in *M. stichopi* Na^+/K^+ *ATPase* expression was not overlapping with *v-ATPase b1* (Fig. 4G). While *v-ATPase b1* was expressed in the gut as shown by coexpression with *plastin* (Fig. 4H, see also Supplementary Fig. S3p for colorimetric expression of *plastin*) and faintly in two proximal lateral posterior rows of cells neighboring the gut, Na^+/K^+ *ATPase* was limited in cells lining the distal part of the epithelial branches of the gut and extending to the subepidermis (Fig. 4G). *V-ATPase b1* was also not coexpressed with *rh; rh* localized in the epidermis (not shown here), cells neighboring the gut as well as in two distal lateral subepidermal rows, adjacent to *v-ATPase b1* expression (Fig. 4I). Finally, *slc4 a* was expressed in scattered subepidermal cells, two distal lateral rows of cells lining the *slc9* expression, which was restricted to the gut (Fig. 4J), as well as dorsolaterally adjacent to the gonads, as shown by a double FISH with *piwi* (77) (Fig. 4K). These results reveal a complexity in the relationship of the expression patterns to each other in *M. stichopi,* similar to what was observed in *I. pulchra.* In particular, the gut-associated domains can be split in the gut epithelium, a region lining the distal part of the gut epithelium and a lateral gut-lining region.

From this analysis, it became evident that in acoelomorphs, the gut-associated domains can be further subdivided into several distinct smaller regions, such as scattered gut-lining cells (both animals), ventral parenchymal mouth-surrounding cells (in *I. pulchra*), the gut epithelium (in *M. stichopi*) or the whole digestive syncytium (in *I. pulchra*) and lateral rows of cells lining the gut (in *M. stichopi*). Overall, these data reveal an unexpected spatial complexity that seems to be unrelated to the presence of an epithelial gut or a syncytium.

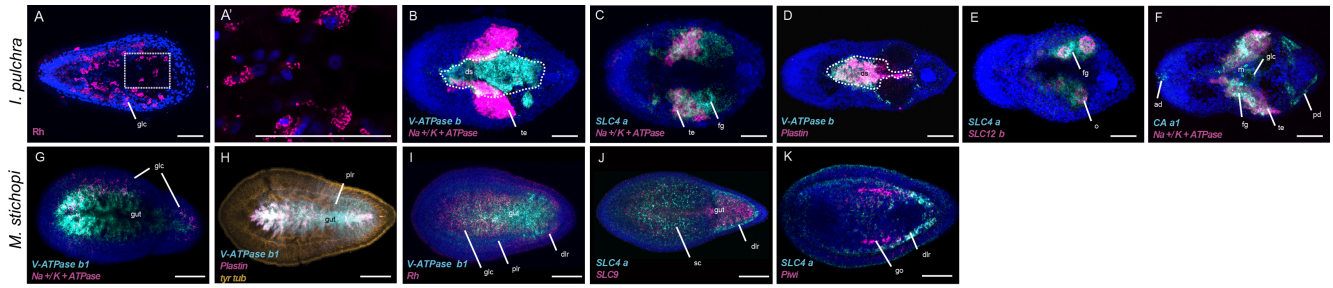

Figure 4. **Rh protein localization by immunohistochemistry and co-expression analysis of excretion-related components by double FISH in *I. pulchra* and *M. stichopi*.** (A) Rh protein localization in *I. pulchra* (B) Relative disposition of *v-ATPase b* and Na^+/K^+ *ATPase* (C) *slc4 a* and Na^+/K^+ *ATPase* (D) *v-ATPase b* and *plastin* (E) *slc4 a* and *slc12 b* (F) *ca a* and Na^+/K^+ *ATPase* in *I. pulchra.* Panel A' shows a higher magnification of the indicated domain in panel A. In panels B and D a white dashed line indicates the digestive syncytium. (G) Relative disposition of *v-ATPase b1* and Na^+/K^+ *ATPase* (H) *v-ATPase b1* and *plastin* (I) *v-ATPase b1* and *rh* (J) *slc4 a* and *slc 9* (K) *slc4 a* and *piwi* in *M. stichopi*. In panel H the cilia and neurons are labeled gold with tyrosinated tubulin. Every picture is a full projection of merged confocal stacks. Nuclei are stained blue with 4',6-diamidino-2-phenylindole (DAPI). Anterior is to the left. ad, anterior domain; dlr, distal lateral rows; ds, digestive syncytium; fg, female gonads; glc, gut-lining cells; go, gonads; plr, proximal lateral rows; lpd, lateral parenchymal domain; o, oocytes; pd, posterior domain; sc, subepidermal cells; te, testis. Scale bars are 50 µm for *I. pulchra* and 100 µm for *M. stichopi*.

Functional analysis of the ammonia excretion mechanism in *I. pulchra.*

To test whether these domains are involved in excretion, we investigated the function of the main ammonia excretion related proteins in *I. pulchra*; Na^+/K^+ ATPase and vacuolar H^+-ATPase a, b proteins -localized in the testis and syncytial cells- and CA A 2 proteins -localized broadly in the parenchyme-. To reveal the putative functional participation of these proteins in ammonia excretion in *I. pulchra* we conducted pharmacological experiments. Adult animals were exposed to commercially available inhibitors targeting Carbonic Anhydrase A 2 (Acetazolamide) (69), v-ATPase a/b (Concanamycin C) (68) and Na^+/K^+ ATPase (Ouabain) (78) in short term experiments (2-3h) and the ammonia excretion rates were monitored. Compared with the control experiments, the ammonia excretion rates were altered to 110%, 80% and 30% when seawater (medium) was enriched with 1 mM Acetazolamide, 5 uM Concamycin C and 1 mM Ouabain, respectively (Fig. 5A), indicating that ammonia excretion is partly occurring via Na^+/K^+ ATPase, thus an active transport mechanism, possibly driven by a v-ATPase. We also used an inhibitor that targets the microtubule network (2mM Colchicine) (79) in order to test whether ammonia excretion involves a vesicular ammonia-trapping mechanism, in which cellular ammonia moves (via membrane diffusion or through Rh-proteins) into acidified vesicles where it gets transformed into its membrane-impermeable ionic form, NH_4, and gets transferred to the membrane through the microtubule network (Fig. 1C). Indeed the relative ammonia excretion rate was reduced to 0,3 (Fig. 5A) suggesting that at least a part of ammonia gets excreted through vesicular transport; possibly in the Rh-expressing cells surrounding the digestive syncytium (Fig. 4A). Finally, we tested whether high environmental ammonia conditions can affect the excretion. Due to the low degree of sensitivity of the electrode to detect small changes in concentration in high environmental ammonia conditions, we monitored the excretion rates after the animals were exposed to various NH_4Cl concentrations. When compared with control experiments, the ammonia excretion rates remained unchanged after exposure to 50 and 100 μM NH_4Cl, but increased gradually after exposure to increasing NH_4Cl concentrations, starting at 200 and 500 μM NH_4Cl (Fig. 5B). This suggests that the ammonia excretion in *I. pulchra* is less efficient in sudden high environmental ammonia conditions, thus ammonia active excretion cannot occur against concentration gradients. Together, these findings show that *I. pulchra* excretes ammonia through a gradient-dependent, active transport mechanism through Na^+/K^+ ATPase and possibly of Rhesus and v-ATPase a, b proteins.

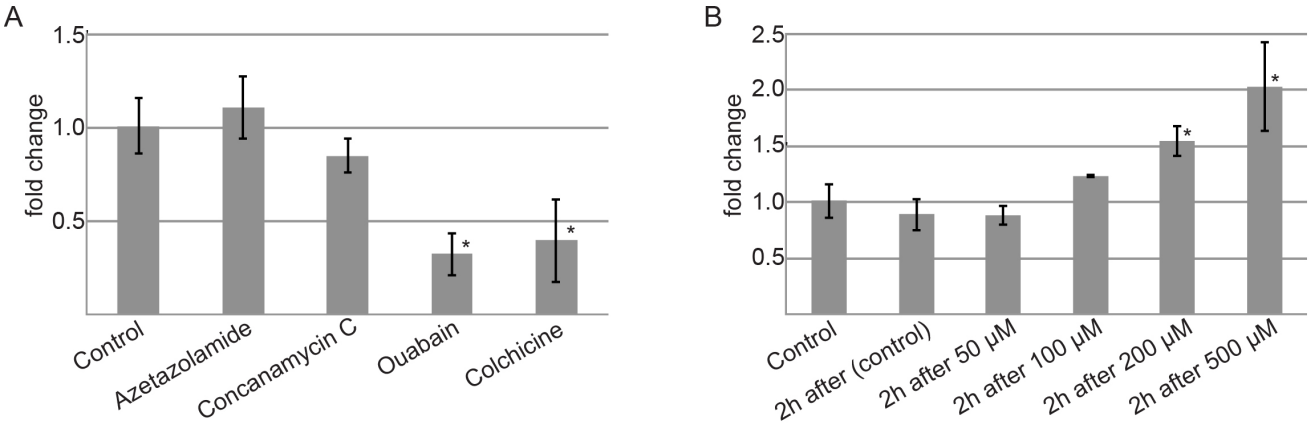

Figure 5. Ammonia excretion rates after exposure to various NH_4Cl concentrations and pharmaceutical inhibitors in *I. pulchra.* (A) Effects of different inhibitors on ammonia excretion rates in *I. pulchra.* The concentrations used were 5 µM Concanamycin C as a v-ATPase inhibitor, 1 mM Azetazolamide as an inhibitor of the Carbonic Anhydrase A 2, 1 mM Quabain as a Na^+/K^+ ATPase inhibitor and 2mM Colchicine for inhibiting the microtubule network. (B) Ammonia excretion rates of *I. pulchra* before (control) and after exposure for 2h to various NH_4Cl concentrations (50, 100, 200 and 500 µM NH_4Cl; N=2 for all treatments). Excretion was measured in the corresponding NH_4Cl concentration (N=2 for each condition).

Identification and characterization of genes involved in ammonia excretion and ultrafiltration site assembly in the cnidarian *Nematostella vectensis.*

To test whether similar putative excretion domains are also found outside bilaterians thus indicating a common excretion mechanism in non-nephrozoans we included in our analysis the anthozoan *N. vectensis* as a non-bilaterian outgroup. We looked for the orthologous excretion-related genes in the genome of *N. vectensis* and found sequences for all genes with the exceptions of nephrin/kirre (Fig. 1). We focused on genes encoding the main ammonia excretion related proteins (rh/amt, Na^+/K^+ ATPase, v-ATPase a, b and carbonic anhydrase A 2, 4) and genes associated with the components of the ultrafiltration site of terminal cells/podocytes in nephridia (zo1 and cd2ap) and examined their expression patterns in juvenile polyps.

Three *rh* copies were revealed in *N. vectensis* genome and their expression was revealed by WMISH and immunochemistry (Fig. 6A-F) *Rh 1* was expressed in individual external cells of the tentacles, other than cnidocytes, the endodermal body wall (gastroderm), the pharynx as well as the lateral part of the mesenteries (Fig. 6A). *Rh 2* exhibited faint expression in the lateral part of the mesenteries and the gastroderm (Fig. 6D). Finally, transcripts of *rh 3* were detected in the gastroderm, the pharynx and the lateral part of the mesenteries (Fig. 6E). Rh protein localization was analyzed in adult animals and it recapitulated the transcript expression pattern in juveniles. In particular, Rh protein was strongly seen in individual cells at the base of the tentacular ectoderm, which resembled gland cells (Fig. 6b), the endodermal body wall and the somatic part of the gonads in the directive mesenteries (Fig. 6C-F). Observations with higher magnification showed that the transporter is localized in vesicles in the cytoplasm of the cells in the lateral part of the mesenteries and the endodermal body wall, similar to

what has been observed in *I. pulchra* (Fig. 6F'). We also looked for the *rh*-related *amts* and seven copies were detected; *amt1, amt2*, *amt3, amt5* and *amt7,* orthologous to *C. elegans amt 2/3,* and *amt4* and *amt6,* orthologous to *C. elegans amt 1/4* (Supplementary Fig. S1). The expression patterns of *amt1, amt2, amt3, amt4*, *amt5* and *amt6* were revealed. *Amt1* was localized all over the gastroderm and so did *amt2* (Supplementary Fig S5a-b). *Amt3* and *amt4* were both expressed in the pharynx and the lateral part of the mesenteries (Supplementary Fig S5c-d). *Amt4* was further expressed in ectodermal cells of the tentacles, other than cnidocytes (Supplementary Fig S5d). The expression patterns of *amt5 and amt6* appeared very similar, demarcating the tentacular ectoderm, the oral ectoderm, the anterior gastroderm and the most posterior part of the gastroderm (Supplementary Fig S5e-f).

Two *Na^+/K^+ ATPase* paralogs were detected in *N. vectensis* genome and both were expressed in a similar fashion, along the lateral domain of the mesenteries, the septal filaments, the pharynx and individual cells of the endodermal wall, resembling endodermal neurons (Fig. 6G). Again, the protein localization of Na^+/K^+ ATPase was also investigated in adult animals and it seemed consistent with the gene expression in juveniles. Na^+/K^+ ATPase was localized in vesicles of the mesenteries (Fig. 6H), nested cells of the septal filaments with an extended cytoplasm (Fig. 6I) and neurons of the endodermal body wall (Fig. 6J).

V-ATPase a expression was distributed along the lateral domain of the directive mesenteries and in the pharynx (Fig. 6K). *V-ATPase b* was detected in the pharynx and distinct cells of the endodermal body wall (Fig. 6L). V-ATPase a/b protein localization was also revealed in adult animals and it resembled the transcript expression in juveniles: v-ATPase a/b was localized in the endodermal body wall and the mesenteries in a filamentous pattern (Fig. 6M-N) as well as in some nested cells of the septal filaments, similar to what was previously observed for Na^+/K^+ ATPase (Fig. 6O).

Seven copies of *carbonic anhydrase A* were found in *N. vectensis* genome and the expression patterns of *ca a1* and *ca a2* (orthologous of *H. sapiens ca a* 1,2,3,5,7,8,13) and *ca a3* (orthologous of *H. sapiens ca a* 4,6,9,12,14) (Supplementary Fig. S1) were revealed in juvenile polyps. *Ca a1* was expressed along the directive mesenteries, including the pharynx and the septal filaments, as well as in cells of the endodermal body wall (Supplementary Fig. S4g). *Ca a2* was localized in distinct external cells of the tentacles, other than cnidocytes, and faintly in the anterior ectoderm and gastroderm (Supplementary Fig. S4h). *Ca a3* was expressed along the lateral region of the mesenteries, the pharynx, distinct cells of the endodermal body wall and distinct external cells of the tentacles, other than cnidocytes (Supplementary Fig. S4i). These data show that in *N. vectensis* the ammonia excretion-related genes are mainly demarcating gastrodermal domains such cells of the endodermal body wall, the directive mesenteries, septal filaments and the pharynx.

The only ultrafiltration-related genes detected in the genome of *N. vectensis* were *zo1, cd2ap* and six copies of *stomatin/podocin*. The expression patterns of *zo1* and *cd2ap* were revealed in juvenile polyps. *Cd2ap* was restricted in the tentacular ectoderm and the oral ectoderm (Supplementary Fig. S4j). *Zo1* was expressed in scattered ectodermal cells at the level of the pharynx (Supplementary Fig. S4f). These results show that the two ultrafiltration-related genes, *zo1* and *cd2ap* are expressed broadly in the ectoderm including the tentacular and oral ectoderm, scattered ectodermal cells in *N. vectensis*.

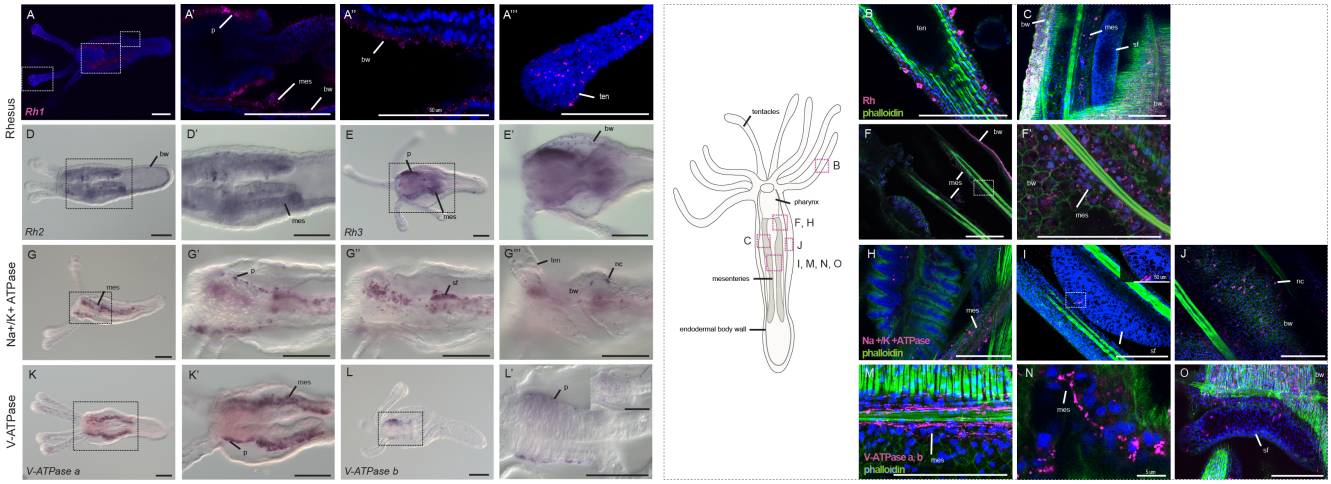

Figure 6. Expression of orthologs of bilaterian ammonia excretion-related components in *N. vectencis.* (A) Whole mount in situ hybridization (WMISH) of *rh 1* (A-A'''), *rh 2* (D-D') *rh 3* (E-E'), *Na$^+$/K$^+$ ATPase* (G-G'''), *v-ATPase a* (K-K') and *v-ATPase b* (L-L') in juvenile polyps, and protein localization revealed by immunohistochemistry of Rh (B-F), Na$^+$/K$^+$ ATPase (H-J) and v-ATPase (M-O) in adult animals. Panels A'-A'', D', E', F', G'-G'', K' and L', show a higher magnification of the indicated domains in panels A, B, C, F, G, K and L, respectively. Anterior is to the left. In panels B-C, F, H-J and M-O the muscle filaments are labeled green with phalloidin. The inset in panel I shows a higher magnification of the indicated domain and the inset in panel L' shows a different focal plane of the animal. Every picture is a full projection of merged confocal stacks. Nuclei are stained blue with 4',6-diamidino-2-phenylindole (DAPI). bw, endodermal body wall; mes, mesenteries; nc, neural cells, ph, pharynx; sf, septal filament; ten, tentacles. The scale bar is 100 µm unless stated otherwise. An illustrated adult *N. vectencis* is provided in the central part of the figure, with the regions shown in panels B-C, F, H-J, and M-O indicated with dashed boxes.

Overall, our findings show that in *I. pulchra, M. stichopi* and *N. vectensis* the ultrafiltration-related genes are expressed broadly indicating that the role of these genes is not related to ultrafiltration. On the contrary, the majority of nephridial tubule-related genes and genes involved in ammonia excretion as well as all the nephridial duct-related genes are mainly expressed in defined domains that are part of or in proximity to their digestive system thus suggesting that in both acoelomorph species and in the cnidarian *N. vectensis* final excretion likely takes place through the gut.

Discussion

The spatial arrangement of the excretory domains in *I. pulchra* and *M. stichopi* is different from the bilaterian nephridial compartments.

Specialized excretory organs such as kidneys and nephridia have been described so far only in Nephrozoa; however most genes associated with individual domains of these organs are also present in non-nephrozoans, and a number of them is also present in unicellular outgroups. In this study we looked for excretion-related genes in the sister group of nephrozoans, the xenacoelomorphs, in order to identify possibly conserved excretory domains, which might have given rise to bilaterian nephridial domains. The analysis of expression patterns of the excretion-related genes revealed a variety of domains with putative excretory functions in this group. The majority of them are neighboring or being part of the digestive system although some individual cells in the periphery, the gonads and the epidermis were also detected. However, in terms of gene expression, these domains seem not to be spatially separated or organized into functionally corresponding domains of nephridia of planarians and vertebrates (Fig. 7A), suggesting that the specialized nephridial cells found in nephrozoans and the putative excretory domains of acoelomorphs are evolutionary not related. Moreover, the fact that these domains do not share significant topological analogies with the nephridial domains suggests that the spatial arrangement of these genes resulting in the formation of specialized excretory compartments (e.g the nephridial compartments) must have taken place after the split of Bilateria into the xenacoelomorphs and nephrozoans.

Ultrafiltration-related genes are expressed broadly in acoelomorphs.

Nephrin/Kirre, Cd2ap, Zo1 and stomatin/podocin proteins have variable biological roles (see supplementary table 1) including the contribution to the podocyte ultrafiltration site of metanephridia in vertebrates (38) and the nephrocyte ultrafiltration diaphragm of insects (39). Nephrin/Kirre genes are also expressed in the ultrafiltration site of terminal cells of protonephridia in planarians (23) and the ultrafiltration diaphragm of rhogocytes in gastropods (4). This conserved expression of ultrafiltration-related genes in the excretion sites of several taxa favors the hypothesis of a common evolutionary origin of ‘ultrafiltration’ excretory cells. However, Cd2ap/Cin85, Zo1 and members of the Stomatin/Podocin are evolutionary ancient proteins present in all Metazoa (47, 48, 80) involved in a number of other functions apart of assembling filtration sites. For instance, stomatin membrane proteins have a role in ion channel regulation and membrane trafficking (81), the MAGUK proteins can be both structural components at the junction sites as well as functioning in signal transduction pathways related to gene expression and cell behavior (82, 83) and the Cd2ap adaptor proteins are

involved in cell signaling, cytoskeletal arrangement and receptor endocytic trafficking (84-87). Nephrin/Kirre cell adhesion proteins are absent outside bilaterians, but present in all Nephrozoa and the non-nephrozoan Xenacoelomorpha (Fig. 1) and are also known to have additional roles except of their participation in filtration site formation such as in myoblast fusion (88), formation of insulin vesicle machinery and pancreatic β-cell survival signaling, synaptic connectivity and formation of the central nervous system and eye development (89-95). In acoelomorphs, Nephrin/Kirre, Cd2ap, Zo1 and stomatin/podocin are expressed broadly including the gonads, parenchymal/subepidermal cells – including possible neurons and muscle cells-, cells lining the digestive tract and cells of the posterior and anterior end (Fig. 7A). So far, ultrastructural data in xenacoelomorphs are not showing ultrafiltration sites, suggesting that the role of these genes is likely not associated with an excretory function in this group. Similarly, we showed that Zo1 and Cd2ap exhibit a broad expression pattern in the cnidarian *N. vectensis,* comprising from tentacular, oral and scattered ectoderm cells. An ectodermal expression of Zo1 has also been reported in *Hydra*, however, in this species transcripts of the gene were distributed in the whole ectoderm (96). Taken all together, it seems that the ancestral function of ultrafiltration-related genes in intracellular interactions and morphogenetic events was coopted for a secondary function in assembling the filtration apparatus of nephridia, nephrocytes and rhogocytes in the Nephrozoa lineage.

In acoelomorphs and cnidarians excretion occurs likely through the digestive tissue.

Interestingly, the majority of the genes analyzed and particularly the ones that are related to ammonia excretion and the nephridial duct are mainly expressed in domains that are part of or in proximity to the digestive system of Acoelomorpha. While this indicates that the final excretion might take place through the gut it remains unclear whether these domains consist of specialized excretory cells or other type of cells (e.g. nurse cells, gland cells) that acquired an additional excretory function. It seems that a degree of sub-functionalization is present, as suggested for example from the distinct expression patterns of *rh* in *I. pulchra*, *aquaporin d* in *M. stichopi* (Fig. 7B). Similarly, in *N. vectensis* almost all ammonia excretion-related genes tested were expressed in cells of the gastroderm, including the lateral domain of the mesenteries and the septal filaments, which have been already proposed to be involved in the transfer of the excretory waste to the exterior (97)). In all three animals, the gut is in direct connection with the environment through the mouth opening and topologically close to most of their surrounding cells and organs. The gut consequently might function as a temporal excrete accumulation cavity before excretes get finally transferred to the environment, possibly combined with defecation. However, their gut architecture differs significantly. *I. pulchra* lacks an epithelial gut and a lumen so the release of metabolites to the environment occurs on an intracellular level (syncytial

cells) (56). The direction of solute and nitrogenous product fluxes would then be from the different surrounding tissues (e.g. gonadal, neuronal, parenchymal) of the animal to the syncytial cells; probably via individual cells such as the gut-lining cells (e.g. Rh or aquaporin a positive). A direction of fluxes towards the syncytium can also be supported by the expression of v-ATPase a, b in the syncytial cells, which forms a proton gradient and thus an acidified environment facilitates the nitrogenous waste transport. On the other hand, both *M. stichopi* and *N. vectensis* possess epithelia-lined guts so excretion takes place on an epithelial level and the metabolites get released into the lumen. In *M. stichopi,* the advantage of having a branched epithelial gut is that it reaches the majority of tissues of the animal resulting in a direct transfer of the nutrients but also of the metabolites from the different tissues to the lumen. However, the tissues that are not in direct contact with the gut need to transfer their excretes to the gut epithelium via transporters of individual cells that surround the gut such as the gut-lining cells (e.g. Rh or aquaporin a, b, c, d positive) or through lateral cellular rows adjacent to the gut epithelium (e.g. aquaporin c positive). The expression of v-ATPase a, b in the gut epithelium is in line with the direction of fluxes towards the gut in *M. stichopi*. Finally, in *N. vectensis,* where a large epithelial gastric cavity extends throughout the body column, the metabolites are likely transferred via transporters of individual cells that populate the endodermal body wall (e.g. Rh positive) and the mesenteries (e.g. Rh and Na^+/K^+ ATPase positive), a domain of the gut particularly enriched in glands and phagocytic cells that serve in digestion and nutrient uptake, towards the lumen. The direction of fluxes towards the lumen can also be supported by the expression of v-ATPase a, b in the endodermal body wall as well as in the septal filaments in *N. vectensis*. A comparison of the three different gut architectures and the proposed direction of fluxes is summarized in Fig. 7B. These observations show that in these three animals, regardless of the gut morphology, their excretion mode use similar principles. They also highlight that these animals have a more elaborated excretory mechanism than just a passive diffusion through the integument, which was previously assumed for some non-nephrozoans due to their loose (e.g. sponges) or epithelial (e.g. cnidarians) cellular organization (1, 20). However, we cannot exclude another, parallel excretion mode through the integument (for example in *M. stichopi amt, rhesus* and *aquaporin e* are expressed in the epidermis).

Excretion through the gut is not an exclusive feature of acoelomorphs and cnidarians, since an excretory role of the gut has been already demonstrated in some nephrozoans. For instance, vertebrates and annelids are excreting nitrogenous products both through their intestine and nephridia (35, 98). Excretion through the digestion tract has also been reported in nephrozoans that lack excretory organs such as in the case of the contractile excretory vesicles near the gut of tunicates (99). Also, the excretory system of insects, tardigrades and arachnids is comprised of malpighian tubules, nephrocytes and different compartments of the gut (e.g. the midgut (100), the hindgut (9) and the

rectum (101)). Due to the high expression of Rh and other ion transporters in the malpighian tubules and parts of the gut, it has been proposed that ammonia and other excretes are firstly secreted into malpighian tubules and then are finally released for excretion in the gut (102, 103), in an analogous way of what is likely the case in acoelomorphs and cnidarians. These observations highlight the importance of the digestive cavity to be confined in close proximity to excretory sites and show how the gut can serve as an excretory device.

The role of Na^+/K^+ ATPase, v-ATPase and Rh/AMT in ammonia–excretion likely predates the Bilateria/Cnidaria split.

Na^+/K^+ ATPase, vacuolar H^+ ATPase and Rh/AMT have a remarkably conserved role in ammonia excretion mechanism within nephrozoans (24-36). In this study we show that the role of Na^+/K^+ ATPase and likely of Rh and v-ATPase a, b in ammonia excretion extends beyond nephrozoans (Fig. 7C). Our functional analysis experiments in acoels confirmed the role of Na^+/K^+ ATPase in ammonia excretion and the proposed mechanism appears very similar to what have been described in other animals (24-26, 28-32, 35, 36, 68, 69, 103, 104). Na^+/K^+ ATPase is expressed predominantly in the testis, adjacently to the digestive syncytium, indicating a putative active ammonia transport from the testis to the gut. It is also possible that a transmembrane ammonia pressure gradient (PNH_3) exists between the gut and the environment, driven partly by the vacuolar H^+ ATPase proton pump, which would facilitate further transport of ammonia through Rh proteins. Moreover, the vesicular protein expression of Rh together with the reduced ammonia rates after short-term perturbation of the microtubule network lead to the suggestion that ammonia is transported in Rh-expressing cells via membrane diffusion into acidified vesicles and then gets transferred to the cell surface by the microtubule network. A similar vesicular ammonia-trapping mechanism has also been shown in the midgut epithelium of the tobacco hornworm (103), the gills of the shore crab (68) and the integument of the nematode (36). Contractile excretory vesicles are also reported near the gut of tunicates (99), free cells of sponges (105) and hydroids (106, 107) but the ammonia transport mechanism is still largely unknown. Similarly, we showed that Rh protein is expressed in vesicles in the endodermal body wall in *N. vectensis*. A transcriptomic comparative study reported an upregulation of a Rh gene in aposymbiotic compared to symbiotic corals, suggesting that it might be involved in ammonium excretion, whereas a second Rh and one AMT gene were upregulated in symbiotic corals compared to aposymbiotic corals suggesting that they might be involved with ammonium supply to their symbion dinoflagellates (108). Moreover, a recent study regarding ammonia excretion in annelids has shown a high abundance of three AMT genes and one Rh gene in their branchiae, organs known to participate in ammonia excretion in these organisms (29). Together, these findings reinforce the conserved role of

Rh/AMT, Na^+/K^+ ATPase and v-ATPase a, b in ammonia excretion and further suggest that vesicular transport of metabolic waste products seems to be used frequently in metazoans as a mean of excretion.

The mode of excretion is not reflecting the body size or the presence of coeloms.

I. pulchra, M. stichopi and *N. vectensis* are relatively small animals without coeloms or internal body cavities and therefore they cannot transport cellular excretes via fluid-filled compartments to their final excretion sites but likely via their gut. The question that arises is whether such mode of excretion, without the presence of specialized excretory organs, is also seen in nephrozoans that lack coeloms and/or also have a small body size. The only group that lack both coeloms and excretory organs are nematodes and nematomorphs (nematoida), in which excretion is assumed to take place through passive and active transport over their body wall (as well as by the taxon-specific renette cell in some nematode taxa) (109, 110). However, platyhelminths, gnathostomulids and gastrotrichs that also lack coeloms but possess protonephridia that ultrafiltrate from the parenchyme. Regarding the body size, even microscopic rotifers, gastrotrichs, micrognathozoans (*Limnognathia maerski*) (111) and miniaturized annelids (*Dinophilus gyrociliatus*) (112) also possess nephridia (protonephridia). Actually, the only other animals lacking excretory organs (apart of nematoida) are the phylogenetically unrelated bryozoans and tunicates. These observations highlight the fact that the presence or absence of excretory organs seem not to relate to the presence or absence of body cavities or to the overall body size but rather to the physiological/ecological adaptation of the animals (nematoids, bryozoans and tunicates) or their phylogenetic position (e.g. acoelomorphs and cnidarians).

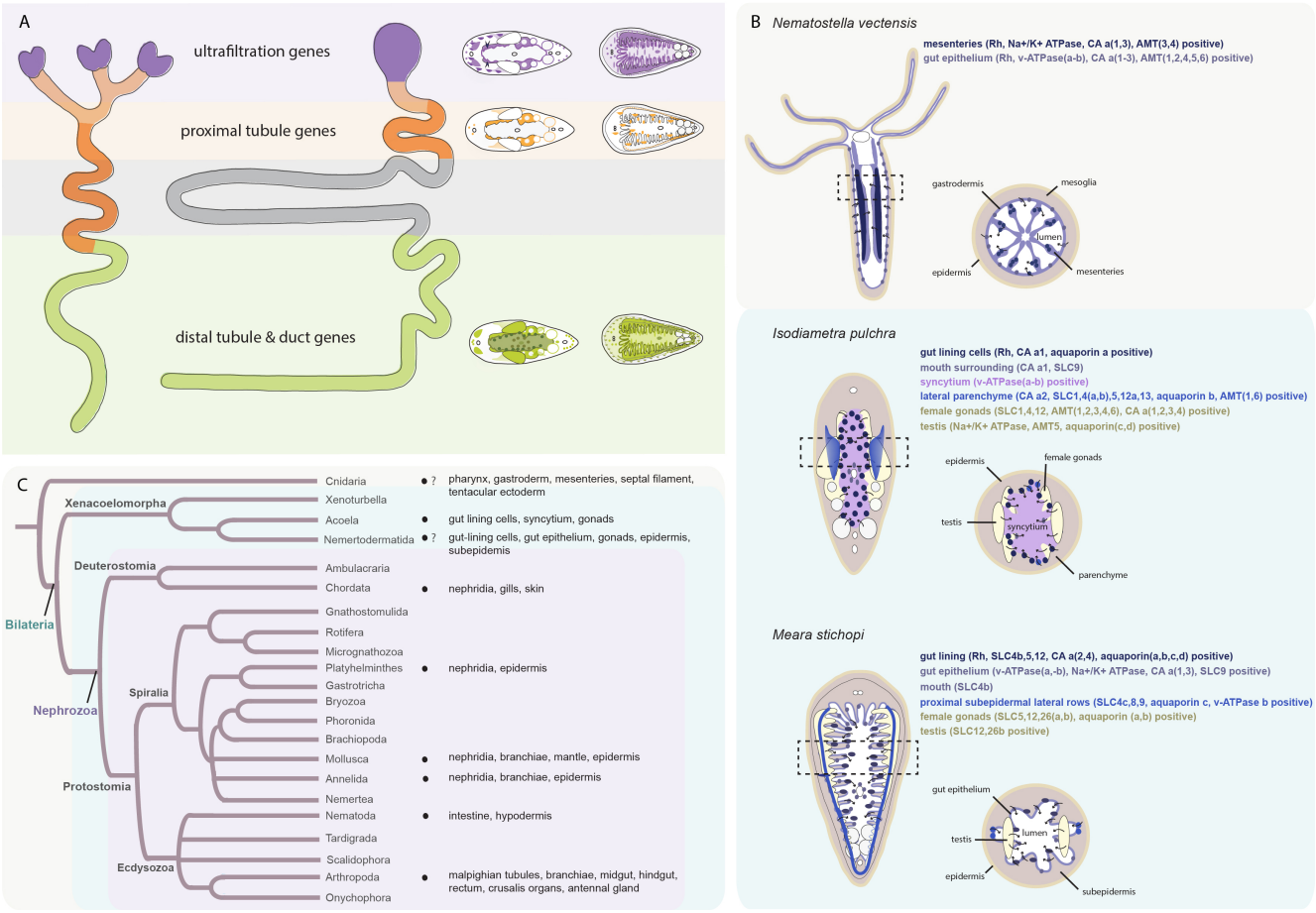

Figure 7. Comparative gene expression profiling of nephridial compartments and putative excretory domains in Acoelomorpha. Illustration of the proposed excretion mode through the gut in *I. pulchra, M. stichopi* and *N.vectensis* and phylogenetic relationships of animals in which a conserved function of ammonia excretion components has been demonstrated. (A) Acoelomorphs putative excretion domains compared to nephridial compartments in terms of gene expression. Orthologous genes marking the main compartments of nephridia don't share significant topological analogies with the excretory domains in acoelomorphs but are mainly expressed in tissues surrounding or associated with the digestive system. (B) Comparison of *I. pulchra, M. stichopi* and *N.vectensis* different gut architectures and proposed direction of fluxes and molecular profiles of the gut and gonad associated domains. (C) Phylogenetic tree compiled on the supplementary table S1 showing the groups (indicated with dots) where the role of Na^+/K^+ ATPase, Rh and v-ATPase a, b in ammonia excretion has been functionally tested and their excretory sites/ organs.

Conclusions

To conclude, these results imply that in the investigated species of Acoelomorpha (*I. pulchra* and *M. stichopi*) and Cnidaria (*N. vectensis*), excretion takes place most likely through the gut, as seen from the molecular profile of digestion-tract associated domains, and not by passive diffusion, as it was previously assumed for non-nephrozoan animals. These domains are not spatially arranged in a corresponding manner to nephridial domains suggesting that they are evolutionary unrelated to nephridia. To understand whether the mode of excretion through the gut represents an ancestral character of animals, ctenophores and sponges need to be included in future studies.

Author contributions

C.A. and A.H. designed the study. C.A., D.T. and A.J.R.S. performed the experiments. C.A. analyzed the data and C.A. and A.H. wrote the manuscript. All authors read and approved the final manuscript.

Acknowledgments

We thank Fabian Rentzsch, Patrick Steinmetz and Hanna Kraus (Sars Centre, University of Bergen, Norway) for kindly providing *N. vectensis* animals and cDNA. Peter Ladurner provided kindly the *I. pulchra* cultures that were kept in the animal facility at the Sars Centre. We also want to thank Chema Martín-Durán and Kevin Pang for improving the manuscript and Anlaug Furu Boddington and other S9 lab members for the help with the collections of *M. stichopi*. The study was supported by the core budget of the Sars Centre, the European Research Council Community's Framework Program Horizon 2020 (2014–2020) ERC grant agreement 648861 to AH (EVOMESODERM), an FP7-PEOPLE-2012-ITN grant no. 317172 (NEPTUNE) to AH and Coca-Cola funding (J.A.R.S.).

References

1. Schmidt-Rhaesa A (2007) *The evolution of organ systems* (Oxford University press, New York).
2. Larsen EH*, et al.* (2014) Osmoregulation and excretion. *Comprehensive Physiology* 4(2):405-573.
3. Locke M & Russell VW (1998) Pericardial cells or athrocytes. *Microscopic Anatomy of Invertebrates*, ed Harrison FWL, M. (Wiley-Liss, New York), Vol 11B:Insecta, pp 687-709.
4. Kokkinopoulou M*, et al.* (2014) 3D-ultrastructure, functions and stress responses of gastropod (*Biomphalaria glabrata*) rhogocytes. *PLoS One* 9(6):e101078.
5. Bradley TJ (1998) Malpighian tubules. *Microscopic Anatomy of Invertebrates* ed Harrison FWL (Wiley-Liss, New York), Vol 11B: Insecta, pp 809-829.
6. Dewel RA & Dewel WC (1979) Studies on the Tardigrades. IV. Fine-Structure of the Hindgut of *Milnesium Tardigradum* Doyere. *Journal of Morphology* 161:79-109.
7. Eichelberg D & Wessing A (1975) Morphology of the malpighian tubules of insects. *Fortschritte der Zoologie* 23:124-147.
8. Greven H (1979) Notes on the structure of vasa Malpighii in the eutartigrade *Isohypsibius augusti* (Murray, 1907). *Zeszyty Naukowe Uniwersytetu Jagiellońskiego* 25:87-95.
9. Phillips JE, Hanrahan J, Chamberlin M, & Thomson B (1986) Mechanisms and Control of Reabsorption in Insect Hindgut. *Advances in Insect Physiology* 19:329-422.
10. Weglarska B (1980) Light and electron microscopic studies on the excretory system of *Macrobiotus richtersi* Murray, 1911 (Eutardigrada). *Cell Tissue Research* 207(1):171-182.
11. Wessing A & Eichelberg D (1975) Ultrastructural aspects of transport and and accumulation of substances in the malpighian tubules. *Fortschritte der Zoologie* 23:148-172.
12. Johnson KE, Perreau L, Charmantier G, Charmantier-Daures M, & Lee CE (2014) Without gills: localization of osmoregulatory function in the copepod *Eurytemora affinis*. *Physiological and Biochemical Zoology* 87(2):310-324.
13. Jondelius U, Ruiz-Trillo I, Baguñà J, & Riutort M (2002) The Nemertodermatida are basal bilaterians and not members of the Platyhelminthes. *Zoologica Scripta* 31(2):201-215.

14. Wilson RA & Webster LA (1974) Protonephridia. *Biological reviews of the Cambridge Philosophical Society* 49(2):127-160.
15. Ruppert EE & Smith PR (1988) The Functional-Organization of Filtration Nephridia. *Biological reviews of the Cambridge Philosophical Society* 63(2):231-258.
16. Bartolomaeus T & Ax P (1992) Protonephridia and Metanephridia - Their Relation within the Bilateria. *Zeitschrift Fur Zoologische Systematik Und Evolutionsforschung* 30(1):21-45.
17. Goodrich ES (1945) The study of nephridia and genital ducts since 1895. *Quarterly Journal of Microscopical Science* 86:113-301.
18. Kümmel G (1962) Zwei neue Formen von Cyrtocyten. Vergleich der bisher bekannten Cyrtocyten und Eröterung des begriffes 'Zelltyp'. *Zeitschrift Fur Zellforschung Und Mikroskopische Anatomie* 57:172-201.
19. Ruppert EE (1994) Evolutionary Origin of the Vertebrate Nephron. *American Zoologist* 34(4):542-553.
20. Willmer EN (1970) *Cytology and evolution* (Academic press, N.Y. and London) 2nd Ed.
21. Raciti D*, et al.* (2008) Organization of the pronephric kidney revealed by large-scale gene expression mapping. *Genome Biology* 9(5):R84.
22. Scimone ML, Srivastava M, Bell GW, & Reddien PW (2011) A regulatory program for excretory system regeneration in planarians. *Development* 138(20):4387-4398.
23. Thi-Kim Vu H*, et al.* (2015) Stem cells and fluid flow drive cyst formation in an invertebrate excretory organ. *Elife* 4:e07405.
24. Cruz MJ*, et al.* (2013) Cutaneous nitrogen excretion in the African clawed frog *Xenopus laevis*: effects of high environmental ammonia (HEA). *Aquatic Toxicology* 136-137:1-12.
25. Gerber L*, et al.* (2016) The Legs Have It: In Situ Expression of Ion Transporters V-Type H(+)-ATPase and Na(+)/K(+)-ATPase in the Osmoregulatory Leg Organs of the Invading Copepod *Eurytemora affinis*. *Physiological and Biochemical Zoology* 89(3):233-250.
26. Hu MY*, et al.* (2013) Development in a naturally acidified environment: Na+/H+-exchanger 3-based proton secretion leads to CO2 tolerance in cephalopod embryos. *Frontiers in zoology* 10(1):51.
27. Mak DO, Dang B, Weiner ID, Foskett JK, & Westhoff CM (2006) Characterization of ammonia transport by the kidney Rh glycoproteins RhBG and RhCG. *American Journal of Physiology - Renal Physiology* 290(2):F297-305.
28. Shih TH, Horng JL, Hwang PP, & Lin LY (2008) Ammonia excretion by the skin of zebrafish (*Danio rerio*) larvae. *American Journal of Physiology - Cell Physiology* 295(6):C1625-1632.
29. Thiel D*, et al.* (2016) Ammonia excretion in the marine polychaete *Eurythoe complanata* (Annelida). *Journal of experimental biology* 220(Pt 3):425-436.
30. Weihrauch D*, et al.* (2012) Ammonia excretion in the freshwater planarian *Schmidtea mediterranea*. *Journal of experimental biology* 215(Pt 18):3242-3253.
31. Weihrauch D & O'Donnell MJ (2015) Links between Osmoregulation and Nitrogen-Excretion in Insects and Crustaceans. *Integrative and comparative biology* 55(5):816-829.
32. Weihrauch D, Wilkie MP, & Walsh PJ (2009) Ammonia and urea transporters in gills of fish and aquatic crustaceans. *Journal of experimental biology* 212(Pt 11):1716-1730.
33. Weiner ID & Verlander JW (2011) Role of NH3 and NH4+ transporters in renal acid-base transport. *Am J Physiol Renal Physiol* 300(1):F11-23.
34. Wood CM*, et al.* (2013) Rh proteins and NH4(+)-activated Na+-ATPase in the *Magadi tilapia* (*Alcolapia grahami*), a 100% ureotelic teleost fish. *Journal of Experimental Biology* 216(Pt 16):2998-3007.
35. Worrell RT, Merk L, & Matthews JB (2008) Ammonium transport in the colonic crypt cell line, T84: role for Rhesus glycoproteins and NKCC1. *American journal of physiology-Gastrointestinal and liver physiology* 294(2):G429-440.

36. Adlimoghaddam A, *et al.* (2015) Ammonia excretion in *Caenorhabditis elegans*: mechanism and evidence of ammonia transport of the Rhesus protein CeRhr-1. *Journal of Experimental Biology* 218(5):675-683.
37. Adlimoghaddam A, *et al.* (2016) Ammonia excretion in *Caenorhabditis elegans*: Physiological and molecular characterization of the rhr-2 knock-out mutant. *Comparative biochemistry and physiology-Molecular & integrative physiology* 195:46-54.
38. Patari-Sampo A, Ihalmo P, & Holthofer H (2006) Molecular basis of the glomerular filtration: nephrin and the emerging protein complex at the podocyte slit diaphragm. *Annual Medicine* 38(7):483-492.
39. Weavers H, *et al.* (2009) The insect nephrocyte is a podocyte-like cell with a filtration slit diaphragm. *Nature* 457(7227):322-326.
40. Abascal F, Irisarri I, & Zardoya R (2014) Diversity and evolution of membrane intrinsic proteins. *Biochimica et Biophysica Acta* 1840(5):1468-1481.
41. Gomes D, *et al.* (2009) Aquaporins are multifunctional water and solute transporters highly divergent in living organisms. *Biochimica et Biophysica Acta* 1788(6):1213-1228.
42. Höglund PJ, Nordstrom KJ, Schioth HB, & Fredriksson R (2011) The solute carrier families have a remarkably long evolutionary history with the majority of the human families present before divergence of Bilaterian species. *Molecular biology and evolution* 28(4):1531-1541.
43. Chan H, *et al.* (2010) The p-type ATPase superfamily. *Journal of molecular microbiology and biotechnology* 19(1-2):5-104.
44. Gogarten JP, Starke T, Kibak H, Fishman J, & Taiz L (1992) Evolution and isoforms of V-ATPase subunits. *The Journal of experimental biology* 172:137-147.
45. Huang CH & Peng J (2005) Evolutionary conservation and diversification of Rh family genes and proteins. *Proceedings of the National Academy of Sciences of the United States of America* 102(43):15512-15517.
46. Smith KS & Ferry JG (2000) Prokaryotic carbonic anhydrases. *FEMS Microbiology Review* 24(4):335-366.
47. Green JB & Young JP (2008) Slipins: ancient origin, duplication and diversification of the stomatin protein family. *BMC Evolutionary Biology* 8:44.
48. de Mendoza A, Suga H, & Ruiz-Trillo I (2010) Evolution of the MAGUK protein gene family in premetazoan lineages. *BMC Evolutionary Biology* 10:93.
49. Srivastava M, Mazza-Curll KL, van Wolfswinkel JC, & Reddien PW (2014) Whole-body acoel regeneration is controlled by Wnt and Bmp-Admp signaling. *Current biology* 24(10):1107-1113.
50. Rouse GW, Wilson NG, Carvajal JI, & Vrijenhoek RC (2016) New deep-sea species of Xenoturbella and the position of Xenacoelomorpha. *Nature* 530(7588):94-97.
51. Hejnol A, *et al.* (2009) Assessing the root of bilaterian animals with scalable phylogenomic methods. *Proceedings. Biological sciences* 276(1677):4261-4270.
52. Cannon JT, *et al.* (2016) Xenacoelomorpha is the sister group to Nephrozoa. *Nature* 530(7588):89-93.
53. Haszprunar G (2015) Review of data for a morphological look on Xenacoelomorpha (Bilateria incertae sedis). *Organisms Diversity & Evolution*.
54. Brusca RC, Moore W, & Shuster SM (2016) *Invertebrates* (Sinauer Associates, Inc., Publishers, Sunderland, Massachusetts U.S.A.) Third edition. Ed pp xix, 1104 pages.
55. Ehlers U (1992a) On the fine structure of *Paratomella rubra* Rieger &; Ott (Acoela) and the position of the taxon *Paratomella Dörjes* in a phylogenetic system of the Acoelomorpha (Plathelminthes). *Microfauna Marina* 7:265-293.
56. Smith JPS & Tyler S (1985) The acoel turbellarians: kingpins of metazoan evolution or a specialized offshoot? *The origins and relationships of lower invertebrates*, ed Conway-Morris S, George, JD, Gibson, R, Platt, HM (Oxford University Press, Oxford).

57. Jondelius U, Wallberg A, Hooge M, & Raikova OI (2011) How the worm got its pharynx: phylogeny, classification and Bayesian assessment of character evolution in Acoela. *Systematic biology* 60(6):845-871.
58. Ehlers U (1992b) Dermonephridia--modified epidermal cells with a probable excretory function in *Paratomella rubra* (Acoela, Plathelminthes). *Microfauna Marina* 7:253-264.
59. Smith JPS & Bush L (1991) Convoluta-Pulchra N-Sp (Turbellaria, Acoela) from the East-Coast of North-America. *Transactions of the American Microscopical Society* 110(1):12-26.
60. De Mulder K*, et al.* (2009) Characterization of the stem cell system of the acoel *Isodiametra pulchra*. *Bmc Developmental Biology* 9.
61. Westblad E (1949) On *Meara stichopi* (Bock) Westblad, a new representative of Turbellaria archoophora. *Arkiv Zoologi* 1:43–57.
62. Børve A & Hejnol A (2014) Development and juvenile anatomy of the nemertodermatid *Meara stichopi* (Bock) Westblad 1949 (Acoelomorpha). *Frontiers in Zoology* 11.
63. Stephenson TA (1935) *The British Sea Anemones* (The Ray Society, London).
64. Fritzenwanker JH & Technau U (2002) Induction of gametogenesis in the basal cnidarian Nematostella vectensis(Anthozoa). *Development genes and evolution* 212(2):99-103.
65. Hejnol A & Martindale MQ (2008) Acoel development indicates the independent evolution of the bilaterian mouth and anus. *Nature* 456(7220):382-386.
66. Genikhovich G & Technau U (2009) In situ hybridization of starlet sea anemone (*Nematostella vectensis*) embryos, larvae, and polyps. *Cold Spring Harbor protocols* 2009(9):pdb prot5282.
67. Chiodin M*, et al.* (2013) Mesodermal gene expression in the acoel Isodiametra pulchra indicates a low number of mesodermal cell types and the endomesodermal origin of the gonads. *PLoS One* 8(2):e55499.
68. Weihrauch D, Ziegler A, Siebers D, & Towle DW (2002) Active ammonia excretion across the gills of the green shore crab *Carcinus maenas*: participation of Na(+)/K(+)-ATPase, V-type H(+)-ATPase and functional microtubules. *Journal of experimental biology* 205(Pt 18):2765-2775.
69. Weihrauch D, Becker W, Postel U, Riestenpatt S, & Siebers D (1998) Active excretion of ammonia across the gills of the shore crab *Carcinus maenas* and its relation to osmoregulatory ion uptake. *Journal of Comparative Physiology B-Biochemical Systemic and Environmental Physiology* 168(5):364-376.
70. Yernool D, Boudker O, Jin Y, & Gouaux E (2004) Structure of a glutamate transporter homologue from Pyrococcus horikoshii. *Nature* 431(7010):811-818.
71. Liao J*, et al.* (2012) Structural insight into the ion-exchange mechanism of the sodium/calcium exchanger. *Science* 335(6069):686-690.
72. Marini AM*, et al.* (2000) The human Rhesus-associated RhAG protein and a kidney homologue promote ammonium transport in yeast. *Nature genetics* 26(3):341-344.
73. Huang CH & Ye M (2010) The Rh protein family: gene evolution, membrane biology, and disease association. *Cell Mol Life Sci* 67(8):1203-1218.
74. Smith JPS (1981) Fine-Structural Observations on the Central Parenchyma in Convoluta Sp. *Hydrobiologia* 84(Oct):259-265.
75. Shinomiya H (2012) Plastin family of actin-bundling proteins: its functions in leukocytes, neurons, intestines, and cancer. *International journal of cell biology* 2012:213492.
76. Zhai L*, et al.* (2016) Argonaute and Argonaute-Bound Small RNAs in Stem Cells. *International journal of molecular sciences* 17(2):208.
77. Stracke K (2012) Expression von Stammzell- und Keimbahn determinierenden Genen in dem Acoelomorphen *Meara stichopi*. (Julius-Maximilians-Universität Würzburg).
78. Lucu C, Devescovi M, & Siebers D (1989) Do amiloride and ouabain affect ammonia fluxes in perfused Carcinus gill epithelia? *The Journal of experimental zoology* 249(1):1-5.

79. Wilson L & Farrell KW (1986) Kinetics and steady state dynamics of tubulin addition and loss at opposite microtubule ends: the mechanism of action of colchicine. *Annals of the New York Academy of Sciences* 466:690-708.
80. Tossidou I*, et al.* (2012) CD2AP regulates SUMOylation of CIN85 in podocytes. *Molecular and cellular biology* 32(6):1068-1079.
81. Lapatsina L, Brand J, Poole K, Daumke O, & Lewin GR (2012) Stomatin-domain proteins. *European journal of cell biology* 91(4):240-245.
82. Bauer H, Zweimueller-Mayer J, Steinbacher P, Lametschwandtner A, & Bauer HC (2010) The dual role of zonula occludens (ZO) proteins. *Journal of biomedicine & biotechnology* 2010:402593.
83. Fanning AS & Anderson JM (1999) PDZ domains: fundamental building blocks in the organization of protein complexes at the plasma membrane. *The Journal of clinical investigation* 103(6):767-772.
84. Harrison BJ*, et al.* (2016) The Adaptor Protein CD2AP Is a Coordinator of Neurotrophin Signaling-Mediated Axon Arbor Plasticity. *Journal of neuroscience* 36(15):4259-4275.
85. Huber TB*, et al.* (2003) Nephrin and CD2AP associate with phosphoinositide 3-OH kinase and stimulate AKT-dependent signaling. *Molecular and cellular biology* 23(14):4917-4928.
86. Johnson RI, Seppa MJ, & Cagan RL (2008) The Drosophila CD2AP/CIN85 orthologue Cindr regulates junctions and cytoskeleton dynamics during tissue patterning. *Journal of cell biology* 180(6):1191-1204.
87. Kobayashi S, Sawano A, Nojima Y, Shibuya M, & Maru Y (2004) The c-Cbl/CD2AP complex regulates VEGF-induced endocytosis and degradation of Flt-1 (VEGFR-1). *FASEB journal* 18(7):929-931.
88. Krauss RS (2007) Evolutionary conservation in myoblast fusion. *Nature Genetics* 39(6):704-705.
89. Kapodistria K*, et al.* (2015) Nephrin, a transmembrane protein, is involved in pancreatic beta-cell survival signaling. *Molecular and cellular endocrinology* 400:112-128.
90. Kuusniemi AM*, et al.* (2004) Tissue expression of nephrin in human and pig. *Pediatric research* 55(5):774-781.
91. Li X & He JC (2015) An update: the role of Nephrin inside and outside the kidney. *Science China-Life sciences* 58(7):649-657.
92. Ramos RG*, et al.* (1993) The irregular chiasm C-roughest locus of Drosophila, which affects axonal projections and programmed cell death, encodes a novel immunoglobulin-like protein. *Genes & development* 7(12B):2533-2547.
93. Strunkelnberg M*, et al.* (2001) rst and its paralogue kirre act redundantly during embryonic muscle development in Drosophila. *Development* 128(21):4229-4239.
94. Wanner N*, et al.* (2011) Functional and spatial analysis of C. elegans SYG-1 and SYG-2, orthologs of the Neph/nephrin cell adhesion module directing selective synaptogenesis. *PLoS One* 6(8):e23598.
95. Zanone MM*, et al.* (2005) Expression of nephrin by human pancreatic islet endothelial cells. *Diabetologia* 48(9):1789-1797.
96. Fei K, Yan L, Zhang J, & Sarras MP, Jr. (2000) Molecular and biological characterization of a zonula occludens-1 homologue in *Hydra vulgaris*, named HZO-1. *Development genes and evolution* 210(12):611-616.
97. Pütter A (1911) *Vergleichende Physiologie* (G. Fischer, Jena).
98. Tillinghast EK (1967) Excretory pathways of ammonia and urea in the earthworm *Lumbricus terrestris*. *Journal of experimental zoology* 166(2):295-300.
99. Burighel P & Cloney RA (1997) Urochordata: Ascidiacea. *Microscopic Anatomy of Invertebrates* ed Harrison FWL (Wiley-Liss, New York), Vol 15, pp 221-347.

100. Nijhout HF (1975) Excretory Role of Midgut in Larvae of Tobacco Hornworm, *Manduca-Sexta* (L). *Journal of Experimental Biology* 62(1):221-230.
101. Butt AG & Taylor HH (1986) Salt and Water-Balance in the Spider, *Porrhothele Antipodiana* (Mygalomorpha, Dipluridae) - Effects of Feeding Upon Hydrated Animals. *Journal of Experimental Biology* 125:85-106.
102. Blaesse AK, Broehan G, Meyer H, Merzendorfer H, & Weihrauch D (2010) Ammonia uptake in *Manduca sexta* midgut is mediated by an amiloride sensitive cation/proton exchanger: Transport studies and mRNA expression analysis of NHE7, 9, NHE8, and V-ATPase (subunit D). *Comparative Biochemistry and Physiology a-Molecular & Integrative Physiology* 157(4):364-376.
103. Weihrauch D (2006) Active ammonia absorption in the midgut of the tobacco hornworm *Manduca sexta* L.: Transport studies and mRNA expression analysis of a Rhesus-like ammonia transporter. *Insect Biochemistry and Molecular Biology* 36(10):808-821.
104. Wall SM & Koger LM (1994) NH+4 transport mediated by Na(+)-K(+)-ATPase in rat inner medullary collecting duct. *The American journal of physiology* 267(4 Pt 2):F660-670.
105. Brauer EB & McKanna JA (1978) Contractile vacuoles in cells of a fresh water sponge, *Spongilla lacustris*. *Cell and tissue research* 192(2):309-317.
106. Schierwater B, Piekos B, & Buss LW (1992) Hydroid Stolonal Contractions Mediated by Contractile Vacuoles. *Journal of Experimental Biology* 162:1-21.
107. Slautterback DB (1967) Coated Vesicles in Absorptive Cells of Hydra. *Journal of Cell Science* 2(4):563.
108. Lehnert EM, *et al.* (2014) Extensive differences in gene expression between symbiotic and aposymbiotic cnidarians. *G3 (Bethesda)* 4(2):277-295.
109. Chitwood BG & Chitwood MB (1950) *Introduction to Nematology* (University Park Press, Baltimore).
110. Turpenniemi TA & Hyvarinen H (1996) Structure and Role of the Renette Cell and Caudal Glands in the Nematode *Sphaerolaimus gracilis* (Monhysterida). *Journal of nematology* 28(3):318-327.
111. Kristensen RM & Funch P (2000) Micrognathozoa: a new class with complicated jaws like those of Rotifera and Gnathostomulida. *Journal of morphology* 246(1):1-49.
112. Kerbl A, Fofanova EG, Mayorova TD, Voronezhskaya EE, & Worsaae K (2016) Comparison of neuromuscular development in two dinophilid species (Annelida) suggests progenetic origin of *Dinophilus gyrociliatus*. *Frontiers in zoology* 13:49.